5-2024

Evaluation of Beach-fx — Beach Nourishment Planning Model – Miami Beach Case Study

Brennan Chase Banks
Florida Institute of Technology, bbanks2018@my.fit.edu

Evaluation of Beach-*fx* — Beach Nourishment Planning Model – Miami Beach Case Study

by

Brennan Chase Banks, E.I.

A thesis submitted to the College of Engineering and Science of
Florida Institute of Technology
in partial fulfillment of the requirements
for the degree of

Master of Science
in
Ocean Engineering

Melbourne, Florida
May 2024

We the undersigned committee hereby approve the attached thesis,
Evaluation of Beach-*fx* — Beach Nourishment Planning Model – Miami Beach Case Study
by
Brennan Chase Banks, E.I.

_____
Gary A. Zarillo, Ph.D., P.G.
Professor
Ocean Engineering and Marine Sciences
Major Advisor

_____
Paul J. Cosentino, Ph.D., P.E.
Professor
Mechanical and Civil Engineering

_____
Stephen Wood, Ph.D., P.E.
Professor
Ocean Engineering and Marine Sciences

_____
Deniz Velioglu Sogut, Ph.D.
Assistant Professor
Ocean Engineering and Marine Sciences

_____
Brian C. McFall, Ph.D., P.E.
Research Civil Engineer
Coastal and Hydraulics Laboratory
U.S. Army Corps of Engineers

_____
Richard B. Aronson, Ph.D.
Professor and Department Head
Ocean Engineering and Marine Science

Abstract

Title: Evaluation of Beach-*fx* — Beach Nourishment Planning Model – Miami Beach Case Study

Author: Brennan Chase Banks, E.I.

Advisor: Gary A. Zarillo, Ph.D., P.G.

Miami Beach, located on the Southeast coast of Florida, is a concerning location for coastal erosion because of the increasing intensity and frequency of tropical storms, nuisance flooding, and accelerated sea-level rise due to climate change. Miami Beach is famous for its beautiful beaches, making it a location of high interest for tourists, citizens, and investors. It is vital for coastal practitioners to accurately model coastal processes, beach evolution, and storm damage during the planning stage of coastal protection projects. The U.S. Army Corps of Engineers developed the Beach-*fx* model as a tool for engineers, planners, and economists to analyze the benefit-to-cost ratio of beach nourishment through probabilistic life-cycle simulations (Gravens and Moser, 2007). This thesis investigates the methodology used by the U.S. Army Corps of Engineers to recommend construction of beach nourishment projects. Hurricanes Matthew and Irma are the two key hurricane events simulated during the period of interest including the 2016 through 2017 hurricane seasons. The one-dimensional cross-shore numerical model, CSHORE (Johnson et al., 2012), is coupled with Beach-*fx* to provide shoreline evolution data through storm events. The results of this study are focused on three study objectives: calculating the error between the averaged beach profile and the trapezoidal representative profile necessary for Beach-*fx* model inputs, Beach-*fx* sensitivity to the depth of closure, and metrics to assess CSHORE and Beach-*fx* model performance. The combination of Beach-*fx* with CSHORE can be an appropriate modeling scheme for Miami-Dade County for the purpose of beach nourishment planning.

Table of Contents

List of Figures

List of Tables

Acknowledgement

I am thankful for the opportunity to undergo this research and complete my Master of Science through the Department of Defense Science, Mathematics, and Research for Transformation (SMART) Scholarship and my Sponsoring Facility, the U.S. Army Corps of Engineers, Jacksonville District. I would like to thank my SMART Scholarship mentor, Martin Durkin, USACE Jacksonville Coastal/Navigation Plan Formulation Section Coastal Planning Technical Lead, for providing data and assisting with concept development, and Rusty Permenter, U.S. Army Engineering Research and Development Center Coastal & Hydraulics Lab, for concept development.

This study is based upon work performed for the 2022 USACE Jacksonville District Miami-Dade County Main Segment Coastal Storm Risk Management study. Any findings, conclusions, or recommendations expressed are those of the author and do not necessarily reflect the views of the USACE.

Dedication

I dedicate my thesis to my family, friends, teammates, coaches, and mentors who have all helped shape my personal, academic, and athletic development. Specifically, my parents, Julius and Yvette Banks, my siblings, Natalia and Justin, and my nephew Broderick. I love you all so much and appreciate you supporting my passion for coastal science and engineering.

Chapter 1
Introduction

Evaluation of Beach-*fx* — Beach Nourishment Planning Model – Miami Beach Case Study is a research thesis utilizing the U.S. Army Corps of Engineers, hereafter referred to as USACE, model Beach-*fx*. Beach-*fx* is a one-dimensional (1D) engineering-economic planning model that analyzes the benefit-to-cost ratio (BCR) of nourishing beaches (Gravens and Moser, 2007). The Monte Carlo probabilistic life-cycle analysis of Beach-*fx* applies a random number of storm events in a 50-year time series and models beach profiles, summed as model reaches, through a cycle of erosion and triggered nourishment events. The 1D cross-shore numerical model, CSHORE (Johnson et al., 2012), is coupled with Beach-*fx* to provide shoreline evolution data.

Beach-*fx* is the primary planning model used in USACE Coastal Storm Risk Management (CSRM) studies that result in recommendations for beach nourishment projects. Recommendations for these projects are ultimately transmitted to Congress through a USACE Chief's Report. Projects may be authorized for construction by the biannual Water Resource and Development Act and funded through congressional appropriation bills. The goal of this study is to validate commonly applied modeling methods used to evaluate beach nourishment planning. The results of this study will be focused around three primary topic areas including, calculating the error between the averaged beach profile and the representative profile necessary for Beach-*fx* model inputs, Beach-*fx*'s sensitivity to the depth of closure, and statistical metrics to assess the model performance of CSHORE and Beach-*fx*. The combination of Beach-*fx* with CSHORE can be an appropriate modeling scheme for Miami-Dade County for the purpose of beach nourishment planning.

1.1 Background

Coastal erosion is a natural and anthropogenic phenomenon that depletes shores of sediment in its littoral system. With over 29% of American citizens residing in coastal areas (U.S. Census Bureau, 2021), it is within the interest of national economic development to provide protection to these areas. USACE was originally formed in 1779, after the Revolution War, and re-established under the Military Peace Establishment Act of 1802 as

the federal agency responsible for designing and maintaining the nation's environmental features. It is within the scope of the USACE Civil Works mission to support community resiliency to storm damage by protecting the nation's tidal and nontidal coastlines.

Beach nourishment is the act of placing new sand onto the beach profile and is a standard method for short-term shore protection and stabilization of eroded beaches. Beach nourishments are initially constructed for a steeper profile that allows for natural wave processes to distribute the sand over time into the equilibrium profile as displayed in Figure 1 below.

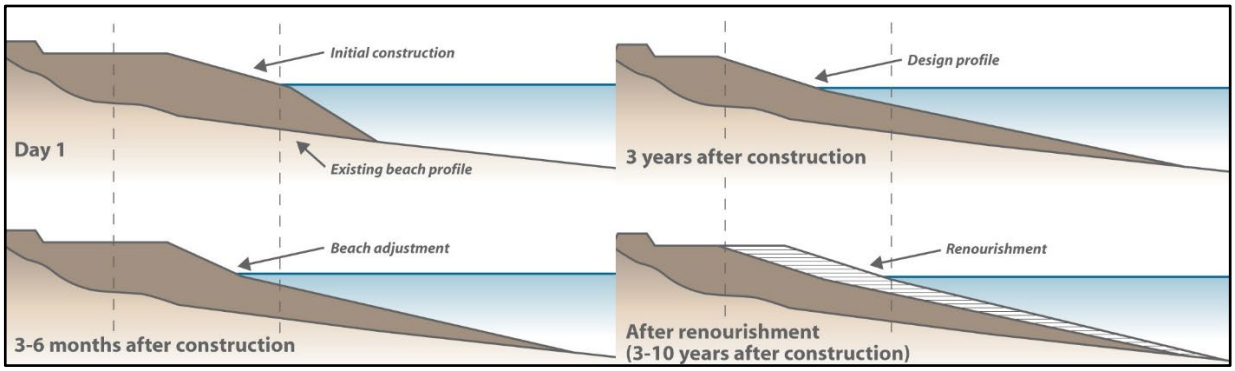

Figure 1: Beach Profile Post Nourishment (USACE Institute for Water Resources, 2007)

Chapter 2

Study Site

Miami-Dade County is located on the Southeastern portion of Florida's coast on the Atlantic Ocean and has a subtropical climate. Miami-Dade County shorelines are barrier island beaches with intricate features such as breakwaters, groins, hardbottom, coral reefs, and erosion hotspots. An erosion hotspot is defined as a section of the coast that exhibits significantly higher rates of erosion than adjacent areas (Kraus and Galgano, 2001). For this study, 46th Street and 55th Street, Miami Beach, were chosen as areas of interest due to their history of nourishment events and designation as erosion hotspots. Figure 2 displays the locations of the 46th Street and 55th Street erosion hotspots at Miami Beach.

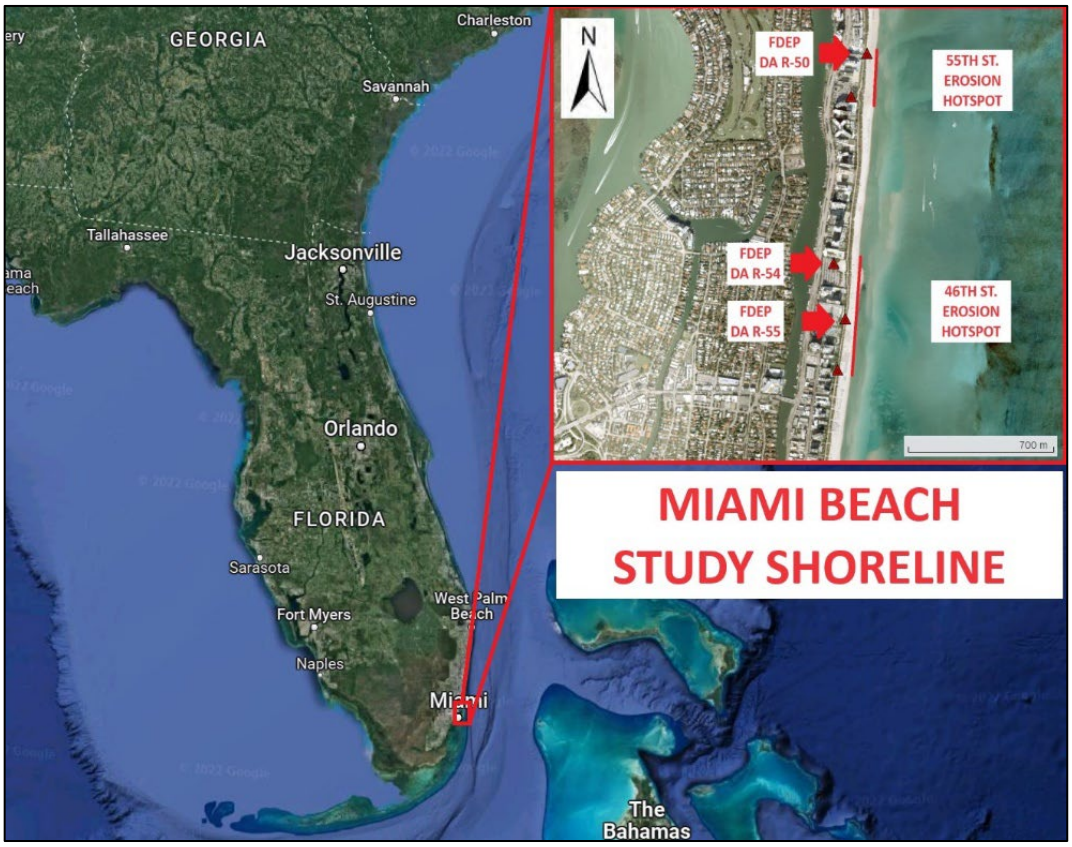

Figure 2: Study Shoreline

2.1 Miami's Coastal Processes

The hydrodynamics of the littoral system are a widely studied area of ocean science and engineering. However, much still needs to be discovered about the incredibly fast-changing area. A great deal of field testing, physical modeling, and numerical modeling research is dedicated to better understanding the processes that define the dynamic movement of coastal lands. The coastal area, or nearshore, is depicted in Figure 3 and is defined as the segment encompassing the inland dune features, the shoreline from high water level to low water level, and out to depth of closure, or the start of the offshore boundary. The nearshore is the primary focus area of this study.

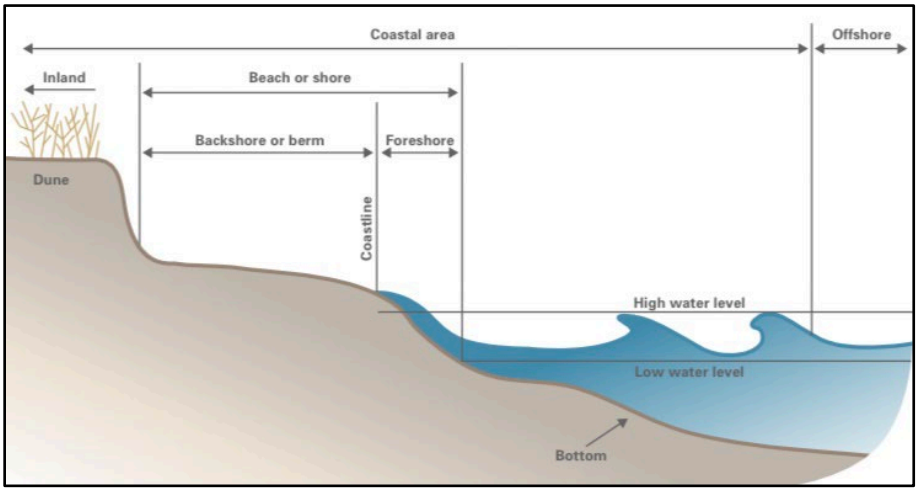

Figure 3: Coastal Boundary Diagram (USACE IWR, 2007)

Coastal processes are the natural occurrences that define the shape and state of the coastline. Morphological changes within the coastal area are primarily due to wind, wave, and current interactions. Sediment transport can be considered in the cross-shore direction, working perpendicular to the beach, and the longshore direction, working parallel along the beach. Sediment may also be transported offshore due to a wave generated undertow. For sediment transport to occur, the forces acting on a particle of sand must be strong enough to disturb the particle from rest. An individual particle of sand will experience three primary forces under steady flow conditions, including the drag force, lift force, and weight (Dean and Dalrymple, 2001). The Depth of Closure (DOC) is the offshore depth beyond which the net sediment transport does not significantly change. The DOC is a critical parameter in

coastal engineering, planning, and design. DOC is especially important in nourishment projects, where the seaward extent of the DOC directly impacts the volume of beach fill (Dean and Dalrymple, 2001).

The Atlantic Coast of the United States experiences high storm activity. High-energy storms such as hurricanes and Nor'easters can cause significant damage to the coastlines. Coastlines are an essential feature to help break wave energy and lessen storm strength prior to reaching critical inland infrastructure and causing severe storm damage. As such, it is vital to uphold the quality of the coastline. Maintaining a healthy beach width and height to protect coastal communities includes placing quality sand on the beach as an act of beach restoration or nourishment. Beach nourishment projects in Florida date back to the early 1940s, followed by more traditional methods gaining popularity in the 1970s. A 2023 Florida Department of Environmental Protection (FDEP) study, shown in Figure 4, reported 686-kilometers (km) of critically eroded beach, including the study site in Miami Beach, 14.5 km of critically eroded inlet shoreline, 143 km of non-critically eroded beach and 5 km of non-critically eroded inlet shoreline statewide (FDEP, 2023).

Figure 4: Florida Critically Eroded Shorelines

2.2 Wind Climate

Winds are a dominant force on coastlines that generate small-amplitude, short period waves, and cause wind driven sediment transport. The USACE Wave Information Study (WIS) Program was developed by the U.S. Engineering Research and Development Center's (ERDC) Coastal and Hydraulics Lab (CHL) and provides reliable data including wind speed and direction offshore of the study site. The WIS wind forcing applies the recommended 10-meter (m) wind fields from the National Centers for Environmental Prediction and National Center for Atmospheric Research (Kalnay et al., 1996). WIS Station 63470 is located closest to the study site approximately 19.3 km east of the project at a depth of 316 m at Mean Sea Level (MSL). The database covers a 40-year span of records from 1980 to 2020. Table 1 provides wind conditions by month over the 40-year record. The predominant wind direction is from the east ranging from 4.8 to 7.1 m. Figure 5 displays the wind rose of Station 63470 with a visual representation of the predominant wind speeds in the cardinal wind directions and the percent occurrence in each direction.

Table 1: Monthly Wind Conditions WIS ST63470

WIS Station #63470 (1980-2020)		
Month	**Average Wind Speed (m/s)**	**Predominant direction**
January	6.8	NE
February	6.5	E
March	7.1	E
April	6.1	E
May	5.5	E
June	4.8	SE
July	4.8	SE
August	4.8	SE
September	5.1	E
October	6.2	NE
November	7.1	NE
December	6.8	NE

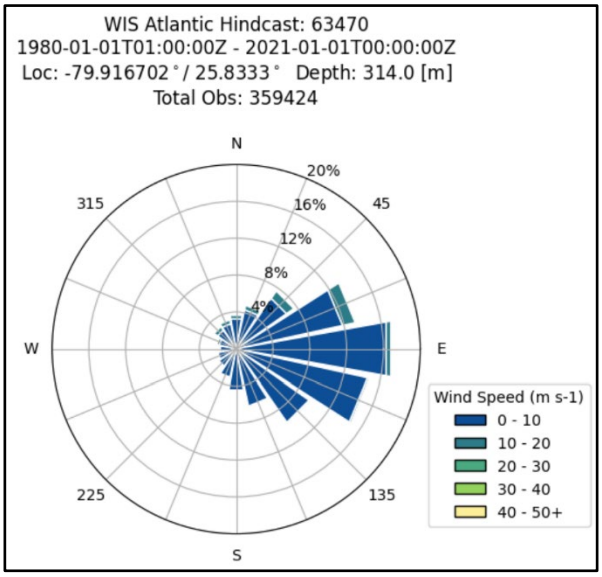

Figure 5: Wind Rose from WIS ST63470

2.3 Wave Climate

The primary method of sediment transport is due to the energy dissipated from breaking waves in the surf zone. The direction of sediment transport is highly influenced by the breaking wave angle (Dean & Dalrymple, 2001). The USACE WIS hindcast database also provides wave data for the Atlantic Ocean. WIS uses the third-generation spectral wave model WAVEWATCH III (Tolman, 2014) to estimate the growth, propagation, and dissipation of ocean waves due to wind forcing. The wind forcing is applied to the selected WIS Station 63470. The WIS data provides a quality overview of the wave climate. However, nearshore wave conditions are likely overestimated due to the high-water depth at the wind station, shoaling, and a nearshore reef system. Table 2 summarizes the monthly average wave height of the WIS waves by direction. Monthly average wave heights range from 0.4 to 1.0 m, indicating a generally mild wave climate year-round. The predominant wave direction is from the northeast. The wave rose in Figure 6 displays a visual representation of the wave climate where the significant wave height is in meters and the percentage occurrences is by cardinal direction.

Table 2: Monthly Wave Climate WIS ST70

WIS Station #63470 (1980-2020)		
Month	**Average Wave Height (m)**	**Predominant direction**
January	0.9	NE
February	0.9	NE
March	0.9	NE
April	0.8	E
May	0.7	E
June	0.4	SE
July	0.4	SE
August	0.4	E
September	0.6	E
October	0.8	NE
November	1.0	NE
December	0.9	NE

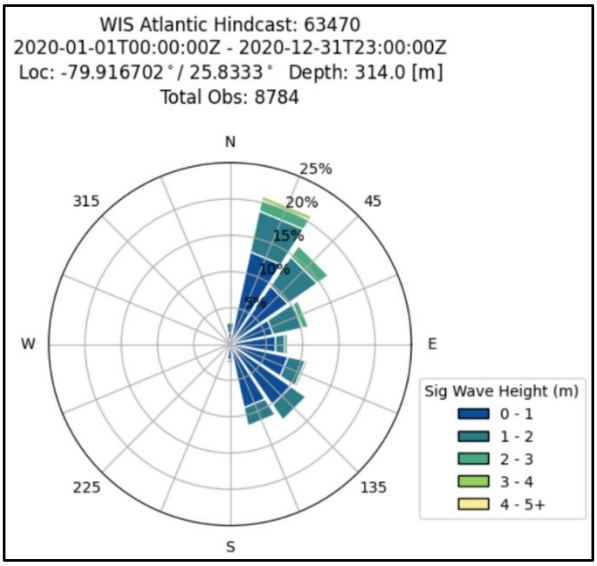

Figure 6: Wave Rose WIS ST63470

2.4 Tidal Influence

Tides are long period shallow water waves that occur due to the gravitational pull of the moon and sun. The magnitude and timing of tides is predictable and has historically been monitored by the National Oceanic & Atmospheric Administration (NOAA) Tides and Currents site. The Tides and Currents site provided tidal datums listed in Table 3 for three locations near the study site at 55th Street and 46th Street Miami Beach. Haulover Pier (Station 8723080) is located directly north of Bakers Haulover Inlet, Virginia Key (Station 8723214)

is located near on the south end of Virginia Key, and finally Vaca Key (Station 8723970) is located Northeast of the Florida Keys and is provided for reference to sea level rise considerations. The tidal range is the difference between Mean High Water (MHW) and mean low water (MLW) and has an average of 0.53 m among the three stations. Figure 7 below displays the proximity of the tide gauges to the study site.

Table 3: Study Site Tidal Datums

Tidal Datum (m) Relative to NAVD88	**Haulover Pier (ST8723080)**	**Virginia Key (ST 8723970)**	**Vaca Key (ST8723970)**
Highest Astronomical Tide (HAT)	0.48	---	0.09
Mean Higher High Water (MHHW)	0.13	0.08	-0.11
Mean High Water (MHW)	0.11	0.06	-0.14
North American Vertical Datum of 1988 (NAVD88)	0.00	0.01	0.00
Mean Sea Level (MSL)	-0.26	-0.26	-0.25
Mean Low Water (MLW)	-0.64	-0.56	-0.36
Mean Lower Low Water (MLLW)	-0.69	-0.60	-0.41
Lowest Astronomical Tide (LAT)	-0.96	---	-0.59

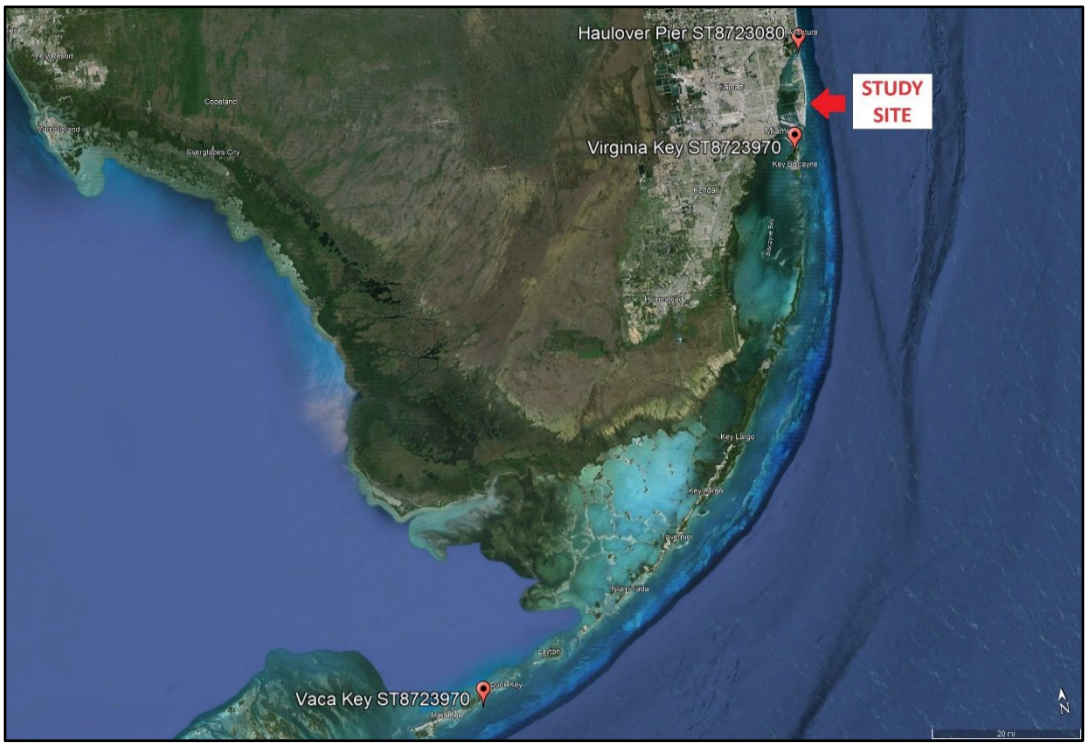

Figure 7: NOAA Tide Stations

2.5 Coastal Geology

The geology of Miami Dade County is dominated by limestone formations and a nearshore consisting of submerged coral reefs and hardbottom reef systems. Miami Beach is a sandy beach on a barrier island composed of poorly graded, fine-grained, white, quartz and calcium carbonate sediment (USACE – Jacksonville District, 2022). The sand has a biogenous origin from coral reef systems. There is a heavy influence from the sand sources of previous nourishment events that must be similar to the original sediment characteristics within a range of set parameters. Coral reefs also provide a great ecosystem service as a natural barrier to dissipate wave energy and serve as highly productive ecosystems supporting tropical fish species. Previous studies in Southeast Florida between Port Everglades Inlet to Bakers Haulover Inlet, about 16 km North of the study area, suggest the nearshore hardbottom promotes strong cross-shore and longshore sediment transport (Lin and Sasso, 1996). According to a Florida Fish and Wildlife Conservation Commission GIS data set, hardbottom is located approximately 762 m from the study shoreline extending out about 2,195 m from the study shoreline. Coral reefs begin directly after the hardbottom and extend approximately 3,048 m from the project shoreline with some additional locations of hardbottom in the area.

2.6 Historical Storm Events

Miami-Dade County is subject to high energy weather events due to its proximity to hurricane-active tropical waters. Hurricanes dominate the shoreline during hurricane season from June through November whereas extratropical events such as Nor'easters occur during the winter and spring months. Storms are known to deteriorate shorelines by eroding beaches and transporting the sediment offshore. Natural beach profiles are eventually restored from storm profiles to a degree with the return of gentle waves (USACE – Institute for Water Resources, 2007). The NOAA National Hurricane Center tracks and records storms on record, and the data is available at the NOAA Digital Coast site. 92 historical storms were tracked within the vicinity of the study area from 1842 to 2022, provided in Figure 8 below. The dotted black circle indicates a 25 nautical mile radius around the study area.

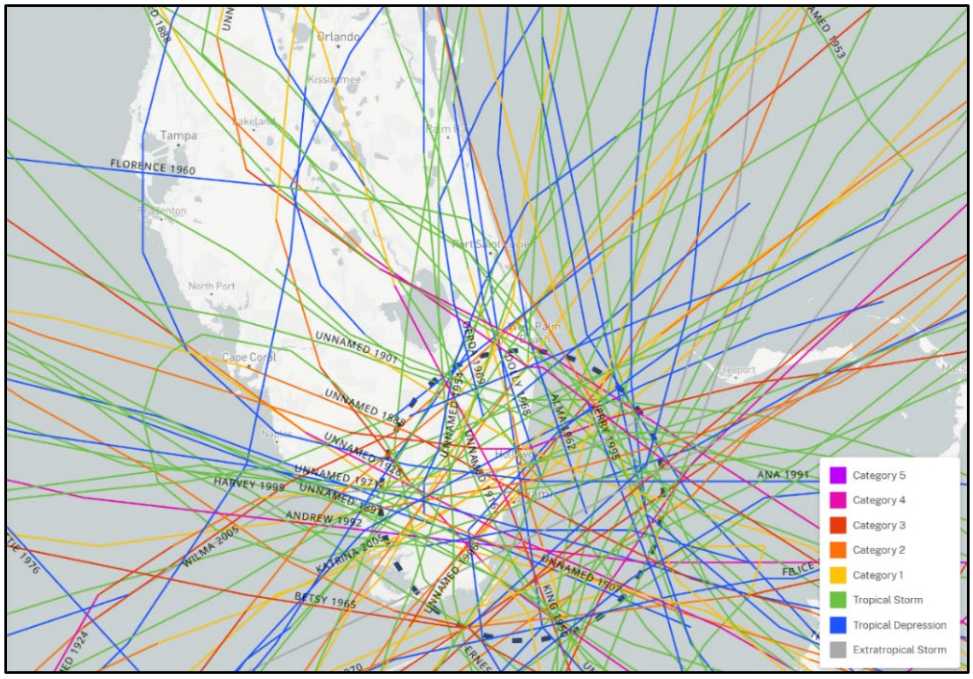

Figure 8: NOAA Historical Storm Track (NOAA, 2022a)

Several recent hurricanes made their mark in history for their storm damage intensity on the Atlantic Coast and the high energy wave climate along Miami-Dade including Hurricane Matthew, a Category 4 Hurricane on the Saffir-Simpson Scale upon passing Miami in 2016, and Hurricane Irma, a Category 3 Hurricane upon impact near Marco Island in 2017. Hurricane Matthew and Hurricane Irma are two storms of interest for this study. Figure 9 below displays the storm tracks of Hurricane Matthew and Irma.

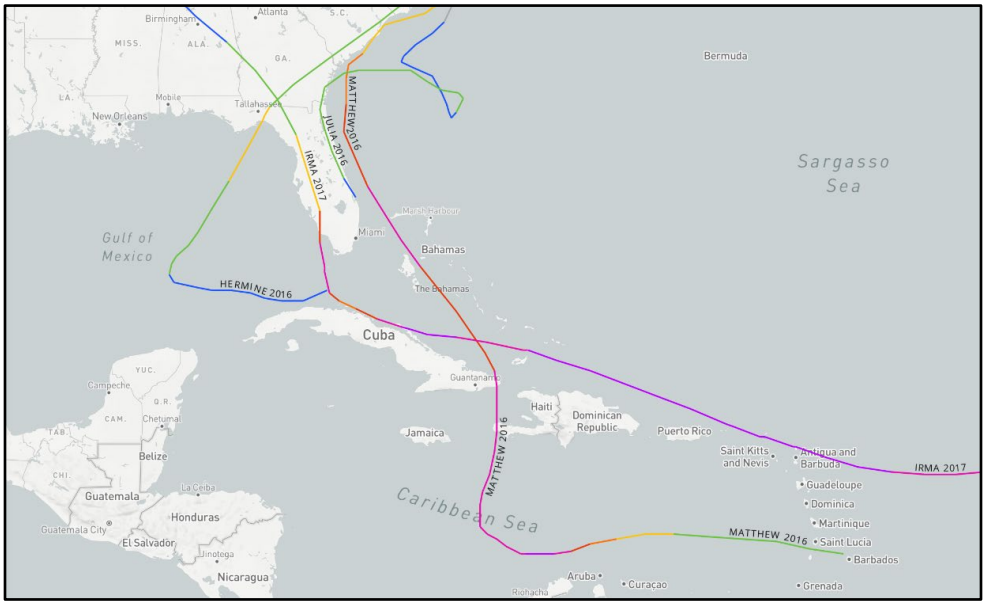

Figure 9: NOAA Historical Hurricane Track 2016 – 2017 Hurricane Season

2.7 Sea Level Rise

Sea levels are anticipated to rise significantly over the next 100 years making sea level rise a vital consideration for any construction project on the coast, especially beach nourishments. Predictions of local Relative Sea-Level Change (RSLC) are available through the USACE RSLC Curve Calculator. The USACE RSLC Curve Calculator methodology is outlined in the Engineer Regulation (ER) 1100-2-8162, Incorporating Sea-Level Changes in Civil Works Programs (USACE, 2019a) and Engineering Pamphlet (EP) 1100-2-1 (USACE, 2019b). A low baseline estimate, an intermediate estimate, and a high estimate are recommended for consideration by the ER 1100-2-8162 methodology. This method utilizes data recorded and validated by NOAA long-term established tide gauges. The Miami Beach gauge is the closest water level gauge; however, it was discontinued in 1981 and the Virginia Key gauge was established nearby in 1994, leaving a large temporal gap. The Haulover Pier and Lake Worth Pier are two stations that are also within the study vicinity but do not provide RLSC trends and prediction scenarios. The Vaca Key gauge (Station 8723970) was chosen to analyze RSLC due to its proximity to the study site and long continuous period of record between 1971 – 2020. The Vaca Key gauge had an observed RSLC trend of 3.95 mm with a 95% confidence interval of 0.45 mm/yr. Figure 10 displays the NOAA RSLC scenario for Vaca Key based on the 2022 Sea Level Rise Technical Report including five scenarios from

low to high predictions along with the 51-year record (1970 - 2021) of observed RSLC. The 2022 Sea Level Rise Technical Report provides sea level rise scenarios to 2150 by decade that include estimates of vertical land motion and a set of extreme water level probabilities for various heights along the U.S. coastline (NOAA, 2022b).

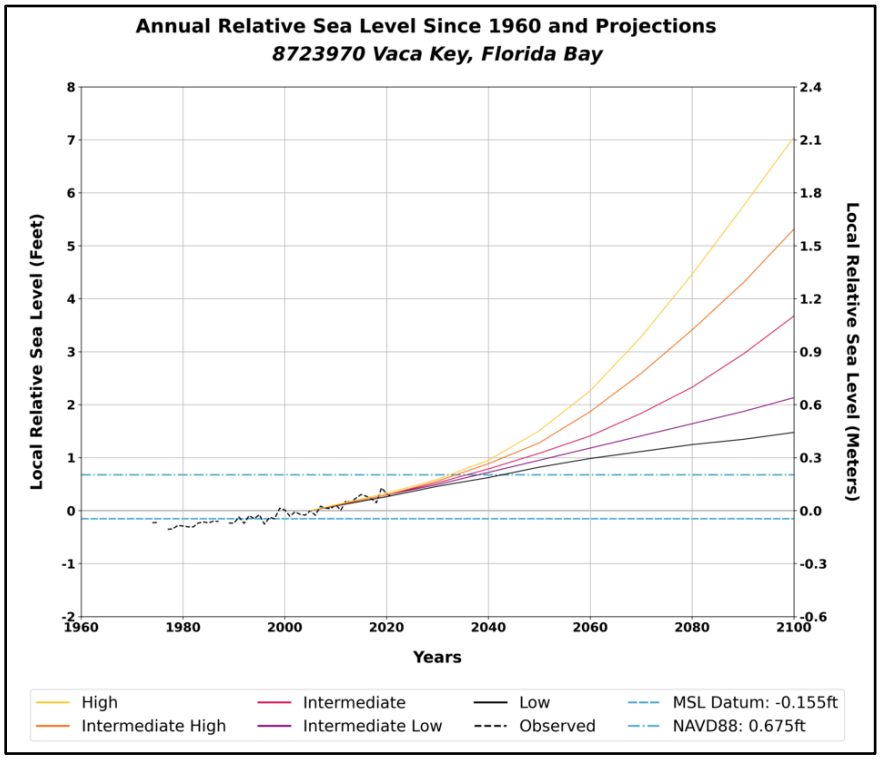

Figure 10: Vaca Key Sea Level Rise Projections

The Southeast Florida Regional Compact Climate Change is a partnership between Broward, Miami-Dade, Monroe, and Palm Beach Counties. The 2019 Compact Unified Sea Level Rise Projection is based on projections of sea level rise developed by the Intergovernmental Panel on Climate Change Fifth Assessment Report as well as projections from NOAA, and accounts for regional effects, such as effects of ice melt, changes in ocean dynamics, vertical land movement, and thermal expansion from warming of the Florida Current that produce regional differences in Southeast Florida's rate of sea level rise compared to global projections. Table 4 provides the 2019 Compact Unified Sea Level Rise Projections up to 2120 in Key West, Florida. (Southeast Florida Regional Climate Change Compact's Sea Level Rise Ad Hoc Work Group, 2019).

Table 4: Southeast Florida Regional Climate Change Compact Sea Level Rise Projection

Year	**Projected SLR (m NAVD88)**
2040	0.16
2070	0.72
2120	2.02

Chapter 3

Previous Studies

Miami-Dade County is under a contract with federal participation from Congress and the USACE Jacksonville District to maintain the barrier island beaches through planned beach nourishment projects. The Florida Beach Erosion Control and Hurricane Protection Projects provides authority for USACE beach nourishment projects and studies under Section 216 of the Flood Control Act of 1970, Public Law 91-611 (33 U.S.C. 549a). The most recent USACE beach nourishment study on Miami Beach was the 2022 Florida Main Segment CSRM. The CSRM was submitted to Congress as a Chief's Report from the U.S. Army Lieutenant General Scott A. Spellmon in September 2022. The CSRM is a comprehensive study including detailed societal impact descriptions, coastal modeling, plan formulation, cost-benefit analysis, an Environmental Assessment, and finally the recommended plan. Datasets used in the 2022 CSRM were provided to assist the completion of this thesis. Airborne Light Detection and Ranging (LiDAR) Digital Elevation Models (DEM) used in the 2022 CSRM are open source from the NOAA Digital Coast office. LiDAR topographic and bathymetric surveys are performed and processed by the USACE National Coastal Mapping Program: Joint Airborne Lidar Bathymetry Technical Center of Expertise (JALBTCX). Surveys are taken around the coastal regions of America before and after significant events such as hurricanes or beach nourishment events including those involved in this study. The 2022 Miami-Dade County, Florida Main Segment CSRM will be widely referenced throughout the thesis study. Further, the modeling methodology used in the thesis will follow those used in the CSRM Engineering Appendix (USACE – Jacksonville District, 2022). A summary of federal nourishment events near the study site up to 2020 is provided in Table 5. The R-Monument Location references the coastal survey range monuments by the FDEP. Figure 11 displays an aerial view of the study area before and after the 2017 erosion hotspot nourishment that placed 136,419 m^3 of sediment on the beach.

Table 5: Previous Federal Nourishment Events

Nourishment Date	R-Monument Location	Volume (m^3)	Length (km)
1979	R-46 to R-58	2,429,100	4
1994	R-55 to R-56	93,350	0.3
1994	R-54 to R-59	22,900	1.6
1996	R-54 to R-60	6,100	2.0
1997	R-54 to R-56	35,000	1.3
1997	R-53 to R-58	26,800	1.0
2007	R-53.5 to R-56	53,500	1.6
2009	R-43 to R-44.5 & 48.7 to R-50.7 & R-53.7 to R-55.5	7,650 & 7,6500 & 2,300	1.4
2012	R-41.5 to R-46.5 & R-53.7 to R-54.7 & R-6.0 to R-6.1	157,800 & 93,460 & 14,470	2.4
2015	R-53.7 to R-55.5	14,720	0.5
2017	R-49 to R-50 & R-53 to R-55.5	64,000 & 114,430	0.6
2020	R-43 to R-46.5 & R-49.5 to R-50.5 & R-53.5 to R-55.5 & R60-R-61	19,100 & 60,250 & 52,300 & 77,140	2.4
Total		~ 3,683,160	~ 19.0

Figure 11: Before and After 2017 Erosion Hotspot Nourishment (USACE - Jacksonville District, 2017)

Chapter 4

Objectives and Study Methods

This thesis study aims to understand further the methods by which USACE plans and recommends a nourishment project using the Beach-*fx* model. Beach-*fx* was developed by the USACE ERDC CHL and is a unique model due to its ability to capture the physical evaluation of beach nourishments, benefits from storm damage reduction, and project costs. The goal of this study is to validate commonly applied modeling methods used to evaluate beach nourishment planning.

This study will focus on a deep analysis of the following three Study Objectives:

1. Comparison of the average morphology profile to the representative profile

A major assumption of Beach-*fx* is the representative trapezoidal beach profile. The average morphology profile simplifies the cross-shore profiles within a defined model reach. A representative trapezoidal profile is constructed by taking idealized dimensions of the average profile across the upland area, dune, berm, and foreshore, which holds less data points and is a less accurate profile. The quality of the trapezoidal assumption will be analyzed by calculating the root mean square error and by method of the coefficient of determination.

2. Beach-*fx* sensitivity to the depth of closure

In practice, there is a high degree of scientific uncertainty in determining the depth of closure (DOC), which may significantly impact the necessary sediment fill volume. The sensitivity to the DOC in Beach-*fx* will be quantified to show the variability in morphology outputs by testing a range of depths, including seven empirical calculations of the DOC and an observed DOC as the true experimental value. Morphology change outputs associated with the different DOC will be compared.

3. Scoring the model performance

Analysis methods help understand the validity and biases of morphodynamic models. The Brier Skill Score (BSS) and Model Bias will be employed in this study to measure the model performance.

4.1 Hypothesis

The combination of Beach-*fx* with CSHORE can be an appropriate modeling scheme for beach nourishment planning in Miami-Dade County. The assumptions made to prepare a representative beach profile for use in Beach-*fx* will have significant error. Beach-*fx* will have a quantifiable sensitivity to the DOC. Both Beach-*fx* and CSHORE will have an acceptable performance for beach nourishment planning.

4.2 CSHORE Overview

Beach-*fx* depends on a cross-shore profile model to create the shore response database (SRD) lookup table to the synthetic storm sweep. This study will utilize CSHORE as the 1D cross-shore shoreline evolution model to predict beach profile response to storm waves and water levels. CSHORE uses linear wave theory to account for sediment transport through the time-averaged continuity, momentum, wave action, and roller energy equations, where a gaussian distribution is applied to the free-surface elevation below MSL (Kobayashi et al., 2009: Johnson et al., 2011). Linear wave theory assumes a small amplitude wave as a homogeneous, incompressible, irrotational, and inviscid fluid (Dean and Dalrymple, 2001). The time-averaged continuity equation [1] is written as:

$$\bar{h}U = q_o \qquad [1]$$

where $\bar{h}$ is the time-averaged water depth, U is the horizontal velocity component acting in the cross-shore direction, and q_o is the wave overtopping rate. The time-averaged momentum equation [2] is written as:

$$\frac{d}{dx}\left(\bar{h}U^2 + \frac{1}{2}g\bar{h}^2\right) = -gS_{bx}\bar{h} - \frac{1}{2}f_b|\bar{U}|U \qquad [2]$$

$$S_{bx} = \frac{dz_b}{dx} \qquad [3]$$

where g is the acceleration due to gravity, S_{bx} [3] is the cross-shore bottom slope, f_b is the bottom friction factor, $\bar{U}$ is the depth averaged horizontal velocity component, z_b is the bed elevation, and x is the cross-shore distance.

The CSHORE sediment transport model computes depth-averaged suspended sediment load [4], q_s, and bed load [5], q_b, based on the undertow current and horizontal velocity component expressed as:

$$q_s = (a\bar{U} + a_o U_o)V_s \qquad [4]$$

$$q_b = \frac{bP_b\sigma_U^3}{g(s-1)}G_s \qquad [5]$$

where a is the suspended load parameter, a_o is the empirical overtopping parameter, U_o is the onshore current caused by the wave overtopping rate, and V_s is the suspended sediment volume per unit horizontal bottom area and is related to the sediment fall velocity and energy dissipation due to bottom friction. In the suspended sediment bed load equation, b is the bedload parameter, P_b is the probability of sediment movement, σ_U is the standard deviation of the horizontal velocity, s is the specific gravity of sand, and G_s is the bottom slope function. The combined wave and current model assume longshore uniformity, uniform grid spacing, and that transects are perpendicular to the shoreline. The effects of a wave roller and quadratic bottom shear stresses are included.

CSHORE has been integrated into a series of MATLAB and Python scripts to prepare inputs including the model reach's bathymetry, storm surge, and associated wave characteristics in the time series, and converts the results into a data file readable by Beach-*fx* (Johnson and Sanderson, 2020). The MATLAB/Python scripts require two input files to provide submerged profile bathymetry and storm information that include the storm date and time, zero moment wave height, mean wave period, and storm surge water elevation. Users may modify input values to adjust the profile, the model domain, and the tidal conditions.

CSHORE outputs the calculated combinations of profiles and storms within a reach. All outputs of the model are time-averaged between the still water level (SWL) and mean sea level (MSL) to predict cross-shore variations of the free surface elevation, the depth-averaged cross-shore current, the cross-shore velocity standard deviation, the cross-shore bed-load transport rate, and the cross-shore suspended sediment transport rate. The root-mean-square wave height, spectral peak period and setup/set down with respect to SWL are used as inputs at the offshore boundary of the computation domain.

4.3 Beach-*fx* Overview

Beach-*fx* is a 1D event-based Monte Carlo simulation model within a Geographic Information System (GIS) framework, used to analyze the BCR of beach nourishment through a life cycle (Gravens and Permenter, In Review). USACE guidance requires CSRM studies to consider risk and uncertainty (USACE, 2019c). Beach-*fx* satisfies this requirement through the probabilistic modeling of risk and uncertainty throughout the study life. The Beach-*fx* application, Version 1.1, is Windows-based with a menu-driven Multiple Document Interface. Beach-*fx* runs a beach profile through a random number of storm events that trigger planned and emergency nourishments over the 50-year life cycle (Gravens et al., 2007). The four primary elements of Beach-*fx* include meteorologic data and processes, coastal morphology change data and processes, economic data and processes, and management measures data and processes. For the purpose of this engineering study, the economic elements will not be considered.

To prepare Beach-*fx* for a new project there are four necessary files including the input database (IDB), output database (ODB), shore response database (SDB), and GIS Directory. The synthetic storm suite is the driver of coastal morphology change in Beach-*fx* and is comprised of a historical record of storms in the study area. Based on the randomly selected storm event from the storm suite, Beach-*fx* will draw from the SRD lookup table based on CSHORE model runs (Kobayashi, 2016). The SRD is a Beach-*fx* generated set of beach profile responses to storms with a range of profile configurations that are expected to exist under different scenarios of storm events and nourishments. From the storm/profile combinations modeled in CSHORE, Beach-*fx* will populate the SRD with the changes in the berm width, dune width, dune elevation, upland width, cross-shore profiles of maximum

erosion, maximum wave height and maximum total water elevation. Beach-*fx* has two management measures to respond to beach erosion including planned and emergency nourishment events. Planned nourishments model federally scheduled and designed beach nourishment projects such as the 2017 USACE hotspot nourishment event. Emergency nourishments model local governments taking action to nourish a profile following a storm event. The outputs include up to 44 ASCII and CSV output files containing model results, error messages, debugging messages, iteration totals, warning messages, and memory usage. The advantage of Beach-*fx* and CSHORE as 1D models is that they are computationally efficient and robust while requiring low time and processing.

Chapter 5

CSHORE Representative Profile Assumption

The nature of a 1D economic-engineering model requires less data in horizontal, vertical, and elevation (X,Y,Z), but makes certain assumptions throughout the model configuration. Beach-*fx* is limited to a simplified representation of beach profiles, or a representative trapezoidal profile, by identifying eight key features outlined in Figure 12, including the upland elevation and width, dune width and height, berm width and height, and dune and foreshore slope. The impacts the representative profile has on Beach-*fx* will be addressed in Study Objective 1, outlined above. Beach-*fx* applies the following assumptions to the trapezoidal profile:

1. Single dune with a constant and equal landward and seaward slope
2. Single berm with constant elevation
3. Static submerged profile
4. Constant foreshore slope
5. Minimum dune elevation equal to the higher of the upland elevation or the berm elevation
6. The upland elevation is constant and the width is greater than or equal to zero

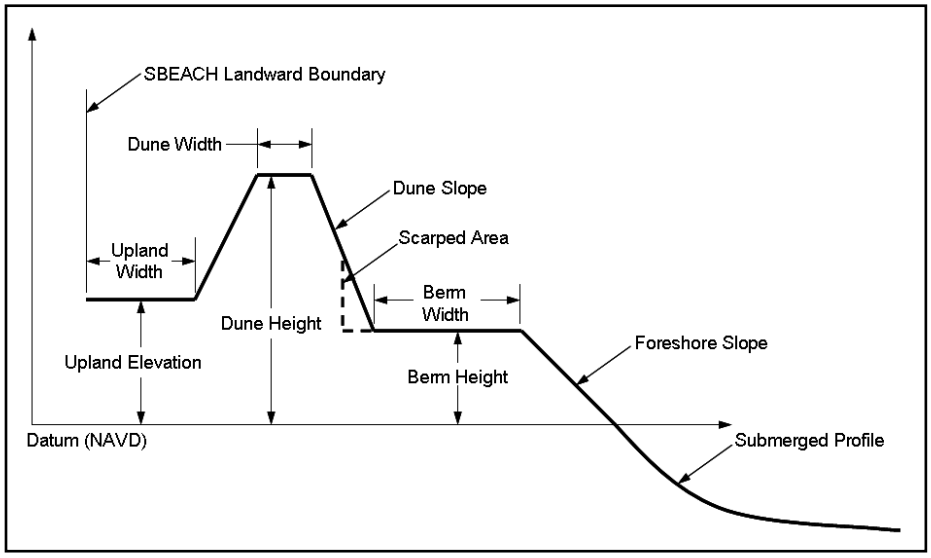

Figure 12: Beach-*fx* Representative Profile Schematic

5.1 Model Reach Creation

The Beach-*fx* project layout is developed by designating model reaches. Model reaches are a section of a coast with constant shore parameters. Reaches used in this study are consistent with the FDEP R-monuments. FDEP R-monuments are spaced approximately 305 m. Within reaches are the individual transect profiles of the shore spaced at 10 m intervals. The study site at the 46th Street and 55th Street Miami Beach erosion hotspot is represented by model reaches 50, 54, and 55 (R-50, R-54, R-55). To ensure no breaching occurs in CSHORE modeling and to be consistent with the Miami-Dade CSRM, 305 m of constant upland elevation was appended to the landward limit behind the back dune toe.

Pre- and post-storm LiDAR surveys were sourced from the NOAA Digital Coast site. Due to a lack in survey data in such a short period of time, the post-Hurricane Matthew and Pre-Hurricane Irma surveys are the same in this study and in the 2022 Miami Dade CSRM. The surveys were processed using USACE JALBTCX toolboxes in Esri ArcGIS Pro including the Dune Feature Extraction Toolbox and the Representative Beach Profile Generator (RBPG) Toolbox. The RBPG toolbox generates a single representative profile for a given study area based on elevation profiles (Spurgeon, 2022). The toolboxes were used to align, and average transects along the model reaches into a single profile based upon NAVD88 as shown in Figure 13. After summarizing the average profile, user inputs across the upland, dune, and berm were input to define the representative trapezoidal profile. The RBPG toolbox determines the RMSE between the user defined representative profile and the average profile. The average RMSE across all profiles is 1.06, which is in an acceptable range for the representative profile.

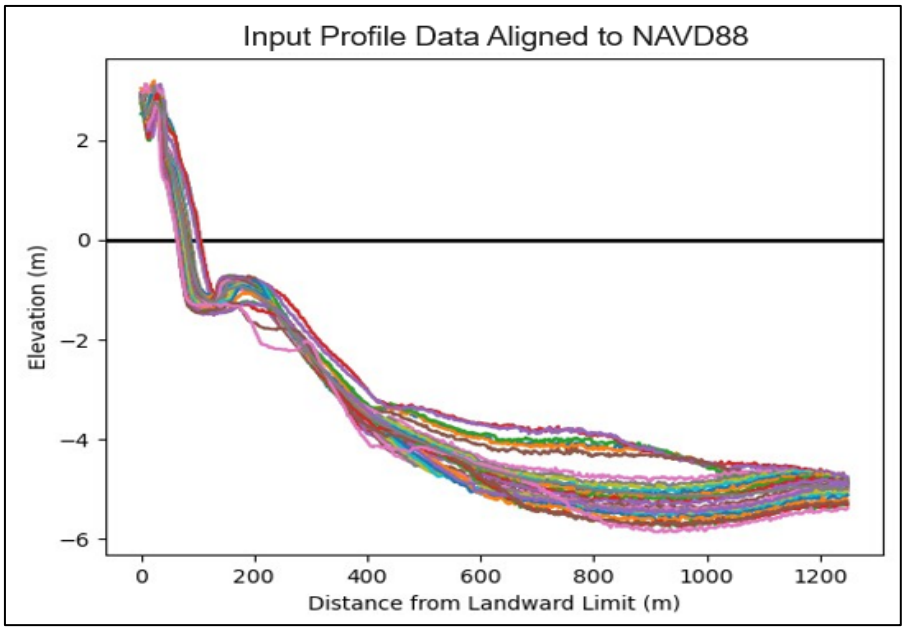

Figure 13: RBPG Toolbox Transect Alignment

The representative profile is only defined above NAVD88. Below NAVD88, Beach-*fx* users have the choice to append the detailed submerged profile (average profile) or the equilibrium profile. The equilibrium beach profile is defined by Dean's 2/3 Power Rule profile and is a function of the mean grain size. The equation for Dean's 2/3 Power Rule [6] is:

$$h(y) = Ay^{\frac{2}{3}} \qquad [6]$$

where h is the depth of the profile, y is distance offshore, and A is the sediment scale parameter. The Miami-Dade Main Segment CSRM (2022) included a detailed geotechnical report that reported a median grain size, d_{50}, equal to 0.47 mm at the study site resulting in a sediment scale parameter equal to 0.1562 $mm^{\frac{1}{3}}$. Three types of profiles were constructed and modeled in CSHORE. Figure 14 provides an example of all three profile configurations for model reach R54 from the 2016 Post-Hurricane Matthew/Pre-Hurricane Irma LiDAR Survey, whereas Figure 15 provides a zoomed in view. Appendix A: Post Processed ArcGIS Profile Summary provides the three profile configurations for each model reach and survey.

1. Average profile (Avg) – The average morphology of the transects within each model reach, sourced from the NOAA LiDAR survey.

2. Representative profile (Rep) – The representative trapezoidal profile with a detailed submerged profile appended below NAVD88.
3. Equilibrium profile (Eq) – The representative trapezoidal profile with the equilibrium profile appended below NAVD88.

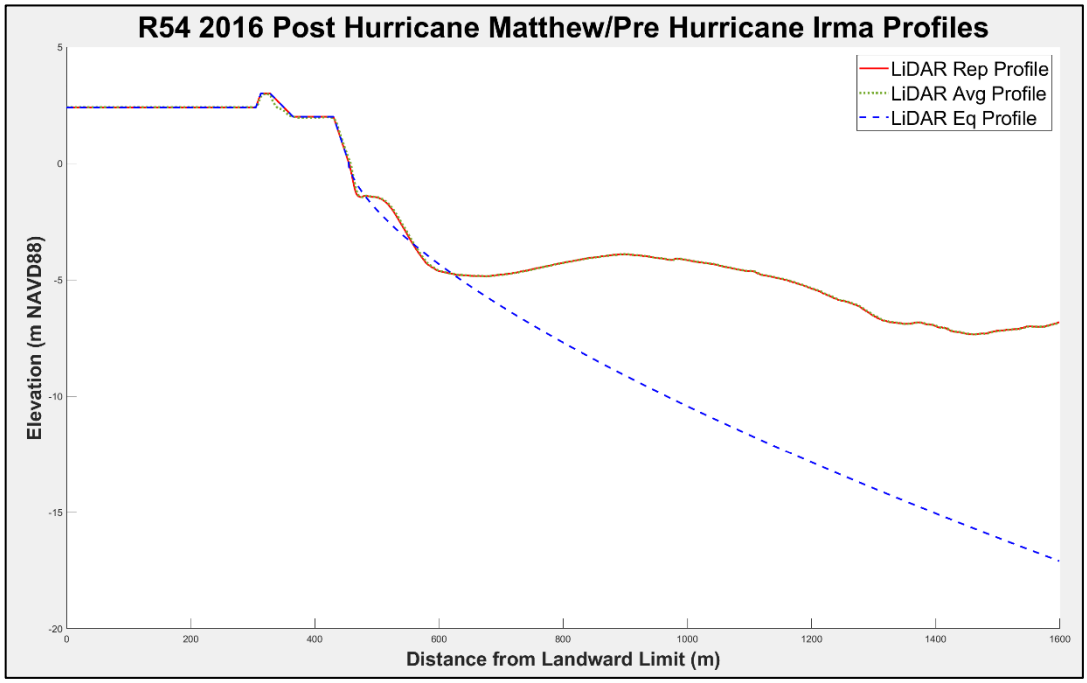

Figure 14: R54 Post-Hurricane Matthew/Pre-Hurricane Irma LiDAR Profiles (Full View)

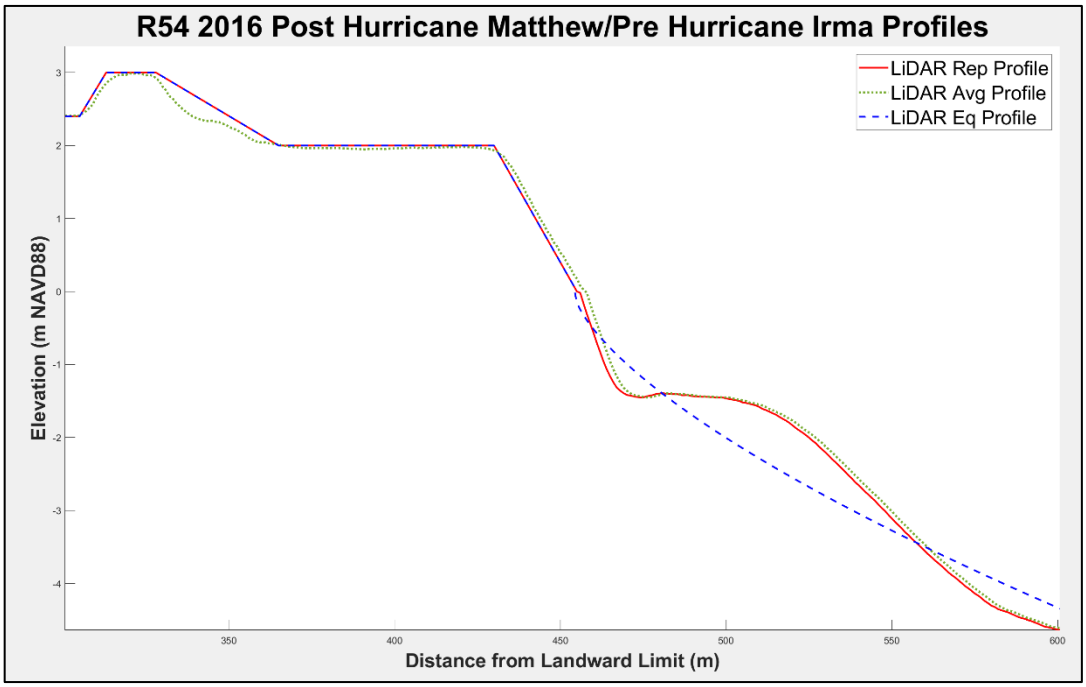

Figure 15: R54 Post-Hurricane Matthew/Pre-Hurricane Irma LiDAR Profiles (Zoomed in View)

The equilibrium profile concaves upwards similarly to natural profiles. However, the *A* scale parameter is dimensional, and it is unable to describe sandbars (Dean and Dalrymple, 2001). In this study the equilibrium profile equated drastically over predicts the depth of the profile. Coarser grain sizes result in steeper equilibrium profiles, indicating that the historical grain size is significantly finer than 0.47 mm. Due to the longstanding history of beach nourishments, there is a high level of uncertainty in the median grain size at Miami Beach. While 0.47 mm may not be descriptive of the average profile, it is the site-specific median grain size measured from the sieve analysis and will continue to be used as the median grain size as it is descriptive of the current study site.

5.2 CSHORE Calibration, Verification, & Data Collection

Calibration and verification are important steps before collection. This is performed by visually comparing post storm survey profiles beach profiles with the modeled shoreline response to storms. CSHORE relies on the user's input to the beach profile, storm data, and input parameters. Storm data for CSHORE and Beach-*fx* were provided by the USACE - Jacksonville District. The CSRM project delivery team (PDT) mined two different datasets

to develop the storm suite including a FEMA synthetic storm suite for tropical storms (BakerAECOM, 2016) which included Hurricane Matthew and Irma. The Ocean Weather Incorporated extratropical analysis was used to develop the extratropical storm suite (Parsons et al., 2018). The storm suite and shore response database were provided by the USACE – Jacksonville District. To account for storms occurring during any combination of tidal phase and tidal range, the peak of each plausible storm surge hydrograph was combined with the astronomical tide at high tide, mean tide falling, low tide, and mean tide rising for each of the three tidal ranges corresponding to the lower quartile, mean, and upper quartile tidal ranges. The storm suite initially included 19 tropical storms and 3 extra tropical storms. CSHORE modeling output create a total of 264 combinations of storm events, each with a corresponding shore response for the entire study site.

Previous ERDC CHL studies produced the recommended range for input parameters (Kobayashi and Farhadzadeh, 2008). Calibration was performed with wave conditions and the average profile for Hurricane Matthew, while verification was performed with a qualitative visual assessment of the average profile for Hurricane Irma. Table 7 provides the range of input parameters valid for CSHORE, and the optimized value obtained from calibration. Figure 16 and Figure 17 display example model calibration and verification run, respectively.

Table 6: CSHORE Calibration Parameters

Input Parameter	**Recommended Range**	**Optimized Value**
Grid size (dx) [m]	1 (field)	1
Median sediment grain size (d_{50}) [mm]	0.15 – 1.51	0.47
Sediment porosity	0.4	0.4
Specific gravity (sg)	2.65	2.65
Suspension efficiency due to breaking (e_B)	0.001 – 0.01	0.002
Suspension efficiency due to bottom dissipation (e_f)	0.01	0.01
Suspended load parameter (a)	0.2 – 0.5	0.2
Bedload parameter (b)	0.0005 – 0.002	0.001

Suspended load parameter for over-topping (slpot)	0.05 – 0.2	0.1
Breaker ratio (ϒ)	0.5 – 0.9	0.5

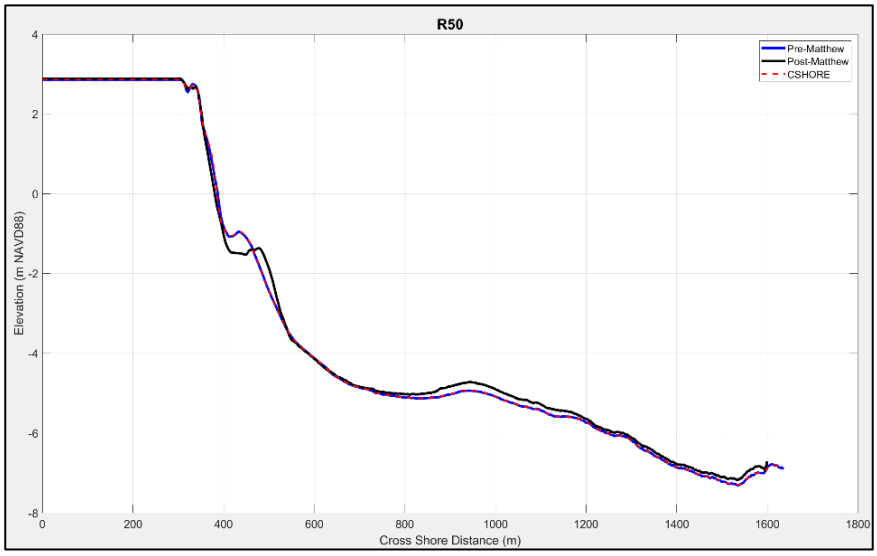

Figure 16: R50 Model Reach Calibration

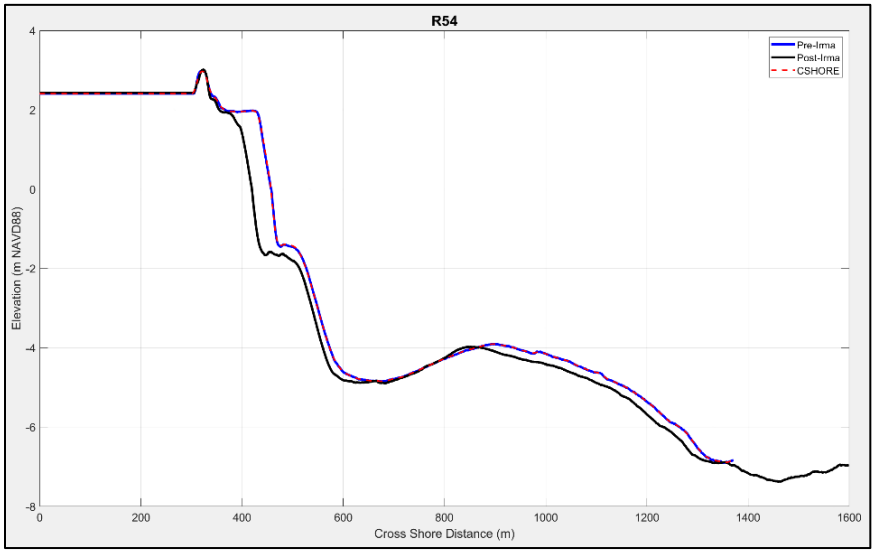

Figure 17: R54 Model Reach Verification

The calibration and verification outputs agreed well at some locations of the profile, but overall CSHORE did not perform well at modeling the post-storm profile. The Miami-Dade CSRM had similar calibration and verification results and was used with confidence for their analysis. Following calibration and verification, the remaining

representative and equilibrium profiles were run in CSHORE for further data collection and analysis. Appendix B: Modeled Profiles provides all model runs for each profile configuration and both hurricane events.

5.3 Statistical Analysis Results

The quality of the representative trapezoidal profile assumption was further analyzed using statistical measures. The upland area behind the landward limit of the dune toe was removed from this analysis to provide better statistical clarity. The area of largest concern in Beach-*fx* is in the dry profile, above NAVD88. To properly consider this area, analysis was also performed between NAVD88 and the landward limit of the dune toe. The root-mean-square error (RMSE) [7] and method of coefficient of determination (R^2) were used to compare post-storm LiDAR survey profiles with modeled profiles, and to compare modeled profiles against each other. The predicted value indicates the post-storm profile bed elevation predicted by the model, whereas the actual value indicates the post-storm profile bed elevation from the average LiDAR survey. The number of data points is represented by *N*, the specific location on the profile is indicated by *i*, and z_b is the bed elevation. The RMSE analysis is an equation used to highlight the accuracy of a model in predicting the target value. The lower the RMSE value is the more accurate the model. Table 7 provides the RMSE for the post-storm LiDAR survey profiles compared to the modeled profiles, while Table 8 provides the modeled profiles compared to each other.

$$RMSE = \sqrt{\frac{\sum_{i=1}^{N}(z_{bPredicted,i} - Z_{bActual,i})^2}{N}} \qquad [7]$$

Table 7: RMSE LiDAR Surveys vs CSHORE Modeled Profiles

Reach/ Hurricane	RMSE (m)					
	Avg LiDAR vs CSHORE		Rep LiDAR vs CSHORE		Eq LiDAR vs CSHORE	
	Full Profile	Dry Profile	Full Profile	Dry Profile	Full Profile	Dry Profile
R50 Matt.	0.58	0.59	0.65	1.08	0.33	1.05
R54 Matt.	2.86	2.4	2.69	1.12	4.07	1.11
R55 Matt.	2.10	1.62	1.94	1.84	2.90	1.82
R50 Irma	1.51	2.32	1.49	1.75	2.20	1.84
R54 Irma	1.69	1.83	1.68	2.31	2.18	2.31
R55 Irma	1.75	1.27	1.59	2.05	2.09	2.04
Average	1.75	1.67	1.67	1.69	2.30	1.695

Table 8: RMSE CSHORE Modeled Profile Comparison

Reach/ Hurricane	RMSE (m)					
	Avg vs Rep		Avg vs Eq		Rep vs Eq	
	Full Profile	Dry Profile	Full Profile	Dry Profile	Full Profile	Dry Profile
R50 Matt.	0.20	0.56	21.01	0.55	20.98	0.06
R54 Matt.	0.48	1.89	21.25	1.89	21.26	0.03
R55 Matt.	0.26	0.88	21. 81	0.88	21.83	0.01
R50 Irma	0.33	1.36	21.43	1.28	21.42	0.11
R54 Irma	0.16	0.34	19.88	0.36	19.87	0.01
R55 Irma	0.35	0.77	20.92	0.73	20.88	0.01
Average	0.30	0.97	21.05	0.95	21.04	0.04

R^2 [8] is a regression statistic that determines how well two datasets correlate. The equation for the linear regression line is represented by $\hat{y}_i$ and the arithmetic mean by $\bar{y}$. A correlation of one indicates perfect correlation, where y is the actual value, $\hat{y}$ is the predicted

value, and $\bar{y}$ is the mean of the y values. The closer the R^2 value is to one, the greater the correlation is between the two datasets. Table 9 provides the R^2 for the post-storm LiDAR survey profiles compared to the modeled profiles, while Table 10 provides the modeled profiles compared to each other.

$$R^2 = 1 - \frac{\sum_i (\hat{y}_i - \bar{y})^2}{\sum_i (y_i - \bar{y})^2} \quad [8]$$

Table 9: R^2 LiDAR Surveys vs CSHORE Modeled Profiles

Reach/ Hurricane	Avg LiDAR vs CSHORE		Rep LiDAR vs CSHORE		Eq LiDAR vs CSHORE	
	Full Profile	Dry Profile	Full Profile	Dry Profile	Full Profile	Dry Profile
R50 Matt.	0.99	0.99	0.99	0.92	0.99	0.92
R54 Matt.	0.96	0.90	0.97	0.85	0.99	0.85
R55 Matt.	0.97	0.92	0.98	0.69	0.99	0.69
R50 Irma	0.98	0.97	0.98	0.75	0.99	0.74
R54 Irma	0.98	0.80	0.98	0.70	0.99	0.70
R55 Irma	0.98	0.86	0.98	0.77	0.99	0.77
Average	0.97	0.91	0.98	0.78	0.99	0.78

Table 10: R^2 CSHORE Modeled Profile Comparison

Reach/ Hurricane	Avg vs Rep		Avg vs Eq		Rep vs Eq	
	Full Profile	Dry Profile	Full Profile	Dry Profile	Full Profile	Dry Profile
R50 Matt.	0.99	0.93	0.93	0.97	0.93	0.99
R54 Matt.	0.99	0.92	0.92	0.92	0.92	0.99
R55 Matt.	0.99	0.95	0.89	0.96	0.89	0.99
R50 Irma	0.99	0.95	0.93	0.95	0.93	0.99
R54 Irma	0.99	0.99	0.92	0.90	0.91	0.89
R55 Irma	0.99	0.93	0.89	0.96	0.89	0.99
Average	0.99	0.95	0.91	0.94	0.91	0.97

5.4 Study Objective 1 Discussion

The CSHORE statistical analysis first measured the modeled post-storm profile and the LiDAR post storm survey. For the RMSE analysis, CSHORE had the overall lowest RMSE value between the representative post-storm profile constructed from the LiDAR survey and the representative post-storm profile modeled in CSHORE. For the full profile, the average RMSE was 1.67 m, and 1.69 m for the dry profile above NAVD88. This indicates that amongst the three profile configurations tested, CSHORE had the lowest error in modeling the post-storm profile for the representative profile. The average profile also had low error values. CSHORE had the highest error in modeling the equilibrium profile. For the R^2 analysis, CSHORE had the overall highest correlation between the average post-storm profile constructed from the LiDAR Survey and the average post-storm profile modeled in CSHORE. For the full profile, the average R^2 was 0.97, and 0.91 for the dry profile above NAVD88. CSHORE had high degrees of correlation for all three profile configurations for the full profile. However, only the average profile had a high correlation when considering the dry profile. CSHORE had the lowest overall correlation in modeling the average profile.

Study Objective 1 was to assess the quality of the representative profile assumption. To address this objective, the modeled profiles are compared against each other. CSHORE had the lowest RMSE value between the modeled average post-storm profile and the modeled representative post-storm profile. For the full profile, the average RMSE was 0.30 m, and 0.97 m for the dry profile above NAVD88. This error is low indicating that the representative profile is a quality representation of the average profile. Due to the vast differences and overprediction of the equilibrium profile, comparing the RMSE with the full equilibrium profile is not valid and ranges from 19.87 m and 21.83 m. However, when considering only the results of the dry profile, the average RMSE was still low. For the modeled average post-storm profile compared to the modeled equilibrium modeled post-storm profile, CSHORE had an average RMSE value of 0.95 m and 0.04 m for the dry representative profile compared to the dry equilibrium profile. The dry representative profile and equilibrium profiles share the same exact trapezoidal dimensions above NAVD88. The low RMSE between the dry representative and equilibrium profiles indicate that despite the overprediction of the depth of the submerged equilibrium profile, there was not enough profile evolution modeled in CSHORE for significant discrepancies to occur in the dry

profile. For the R^2 analysis, CSHORE also had the highest correlation between the average and representative profiles modeled in CSHORE. For the full profile, the average R^2 was 0.99, and 0.95 for the dry profile above NAVD88. CSHORE had high correlation for all three profile configurations for the full and dry profile. CSHORE had the lowest overall correlation between the average and equilibrium profiles. The RMSE and R^2 analyses show that the representative profile is a quality assumption and can be used with confidence to represent the average morphology.

Chapter 6

Beach-*fx* Sensitivity to the Depth of Closure

Beach-*fx* defines the DOC as the depth below the datum to which nourishment material is distributed (Rogers et al., 2009). In this study, the DOC will be considered for several cases as outlined in Study Objective 2. The empirically calculated, or predicted, DOC values, and methodology for determining an observed DOC will follow the equations discussed below.

6.1 Depth of Closure

A new DOC occurs with each passing wave set, making it increasingly difficult to consider the extent of sediment transport in numerical models such as Beach-*fx*. The predicted DOC values are calculated using wave statistics from WIS ST4370 following the methodology outlined in Brutsché et al. (2016). Hallermeier (1978, 1981) [9] [11] was the first to develop an equation for the DOC by using a wave tank to physically model the equilibrium of a beach profile and observe the DOC as a cut depth, h_c. The inner limit DOC is the seaward extent of the littoral zone where the bed experiences extreme activity caused by waves breaking and their related currents (Dean and Dalrymple, 2001). The Hallermeier inner DOC may be written as:

$$h_c(t) = 2.28H_e(t) - 68.5\left(\frac{H(t)_e^2}{gT(t)_e^2}\right) \qquad [9]$$

where H_e is the significant wave height, g is the acceleration due to gravity, and T_e is the significant wave period. H_e is expressed by:

$$H_e = \overline{H_s} + 5.6\sigma_s \qquad [10]$$

$\overline{H_s}$ is the annual average significant wave height and σ_s is the standard deviation of the significant wave height. Combining with equation [9], the Hallermeier inner simplified DOC may also be written as:

$$d_l = 2\overline{H_s} + 11\sigma_s \quad [11]$$

The outer limit which signifies the limit of the shoal zone. Seaward of this point waves will cause little sediment transport. The Hallermeier outer DOC is calculated as:

$$di = (\overline{H_s} - 0.3\sigma_s)\overline{T_s}(\frac{g}{5000D})^2 \quad [12]$$

where $\overline{T_s}$ is the average wave period of the annual mean significant wave height and *D* is the median sediment grain size, or d_{50}. Birkemeier (1985) used field measurements at the ERDC CHL Field Research Facility in Duck, North Carolina to update the inner DOC, defining the Birkemeier inner DOC as:

$$h_c = 1.75H_e - 57.9(\frac{H_e^2}{gT_e^2}) \quad [13]$$

Birkemeier's inner simplified DOC is written as:

$$d_I = 1.57H_e \quad [14]$$

Houston (1995) [15] and Kraus et al. (1999) [16] also developed equation for the DOC that incorporate the annual average significant wave height.

$$h_c = 6.75\overline{H_s} \quad [15]$$

$$h_c = 8.9\overline{H_s} \quad [16]$$

Robertson et al., (2007) developed a methodology for extracting an observed DOC from pre- and post-Hurricane Frances LiDAR surveys in south Florida using Hallermeier (1978) ± 0.3 m closure criteria. To accurately represent the Beach-*fx* model start year of 2016, the observed DOC was obtained for this study by measuring the elevation change grid between the pre- and post-Hurricane Matthew surveys at R50, R54, and R55. Figure 18 displays the elevation change grid with the ± 0.3 m closure criteria and location of closure (LOC). The average observed DOC between R50, R54, and R55 was taken as the observed DOC for the study area. Table 11 provides the observed DOC data from the Hurricane Matthew LiDAR surveys. The ± 0.3 m closure criteria resulted in the same DOC value as the Hallermeier

simplified inner DOC. Similarly, both Birkemeier equations resulted in the same DOC. Ultimately six DOC values were tested in Beach-*fx*. Table 12 provides the eight DOC values that will be tested in Beach-*fx*.

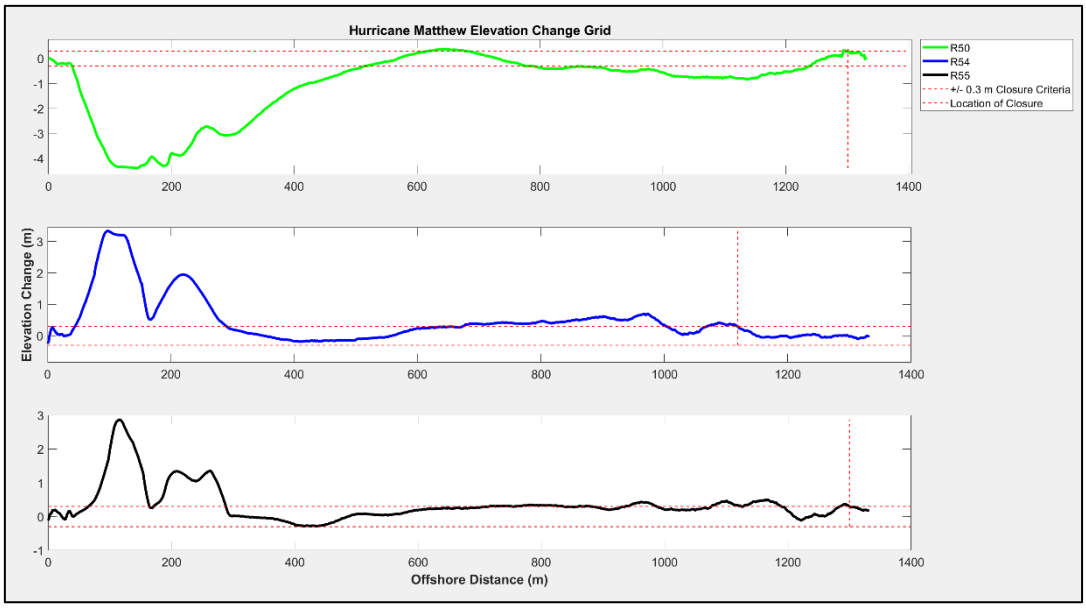

Figure 18: Study Site Elevation Change Grid

Table 11: Observed DOC

Reach	DOC (m)	LOC (m)
R50	6.93	1302
R54	7.31	1119
R55	7.11	1300
Average	7.12	1240
STDEV	0.23	105

Table 12: Tested DOC Values

Predicted DOC							Observed DOC [m]
Hallermeier Inner (1978) [m]	**Hallermeier Inner Simplified (1981) [m]**	**Hallermeier Outer (1981) [m]**	**Birkemeier Inner (1985) [m]**	**Birkemeier Inner Simplified (1985) [m]**	**Houston (1995) [m]**	**Kraus (1999) [m]**	
6.66	7.04	4.73	5.05	5.15	4.12	5.43	7.12
Maximum		7.12		**Average**		5.40	
Minimum		4.12		**STDEV**		1.02	

6.2 Beach-*fx* Calibration, Setup, & Data Collection

The Beach-*fx* calibration procedure is outlined in Gravens and Permenter (In Review). The Miami Beach Main Segment CSRM Appendix A: Engineering discusses the specific steps the Jacksonville District took to calibrate Beach-*fx*. The historical background change rate is a value calculated from historical beach surveys in Miami-Dade County dating back to 1873. Beach-*fx* is calibrated when the model returns the historical background change rate as the sum of the storm induced change rate and the calibrated applied erosion rate (AER) on a reach-by-reach basis. To achieve this, Beach-*fx* was run for 300 iterations and the AER is adjusted until the historical background change rate is achieved. Table 14 provides the calibrated AER values for each model reach.

Table 13: Calibrated AER Values

Model Reach	Historical Shoreline Rate of Change (m/yr)	Storm Induced Change Rate (m/yr)	Calibrated AER (m/yr)
R50	3.00	0.42	2.59
R54	3.73	0.40	3.34
R55	2.65	0.12	2.53

The storm suite of 264 synthetic storms is the predominant driving force for coastal morphology in the model and is developed during the CSHORE modeling portion of the study. Tropical and extratropical storms are contained to specific storms seasons and are

given a probability of occurrence within the season. Tropical storm season is between June 1st and November 30th, while extratropical storm season is between December 1st and May 31st.

The 2022 Miami Dade CSRM PDT model a large range of nourishment scenarios to determine which nourishment configurations provide the best BCR. Table 15 describes the five scenarios selected based on major decision points in the 2022 Miami Dade CSRM. Each nourishment plan is performed once a nourishment in triggered in Beach-*fx*. Planned nourishments are triggered at 1% volume loss to the berm width, dune width, and dune height each. The sum of the necessary fill volume for the study area must be greater than the mobilization threshold volume (2.3 MCM). If triggers have been met at an annual checkpoint interval, Beach-*fx* restores the necessary sediment volume to the design template of the model nourishment scenario. The future without project scenario models the life cycle without any nourishment considerations and is the first scenario modeled by the PDT to use as the baseline. The tentatively selected plan is one of the first major decision milestones and is selected based on the BCR of modeled scenarios at that point in the study timeline. Scenarios were optimized to include a variation of nourishment configurations throughout the study site. The final recommended plan is included in the Chief's Report provided to congress. For each nourishment scenario, six DOC values were tested for a total of 30 model runs, 9,000 iterations, and roughly 300 computation hours.

Table 14: Nourishment Scenarios

Scenario	Nourishment Level	Model Reach	Dune Crest (m)	Dune Width (m)	Berm Width (m)
Future Without Project	R50 to R55	--	--	--	--
Tentatively Selected Plan	Small Nourishment	R50 to R55	31	66	82
Final Recommended Plan	**Medium Nourishment**	**R50 to R55**	**31**	**66**	**164**
Optimization 1 R50 & R54;R55)	Small Nourishment	R50 and R54; R55	36; 36	197; 131	82; 82
Optimization 2	Varied Nourishment	R50 and R54; R55	36; 36	197; 131	131; 131

6.3 Sensitivity Analysis Results

Beach-*fx* sensitivity to the DOC was analyzed by comparing morphology change outputs and metrics including the total number of triggered nourishments, total nourishment volume, the buffer width (BW), and the total erosion volume. The BW is an approach to quantify the resilience created from dune and beach nourishments using Beach-*fx* output metrics (Durkin and Chambers, 2019). For each analysis metric the sum for the entire 300 iteration was taken and averaged between the three model reaches R50, R54, and R55. Figures 19, 20, 21, and 22 display the analysis metric for each scenario per DOC value.

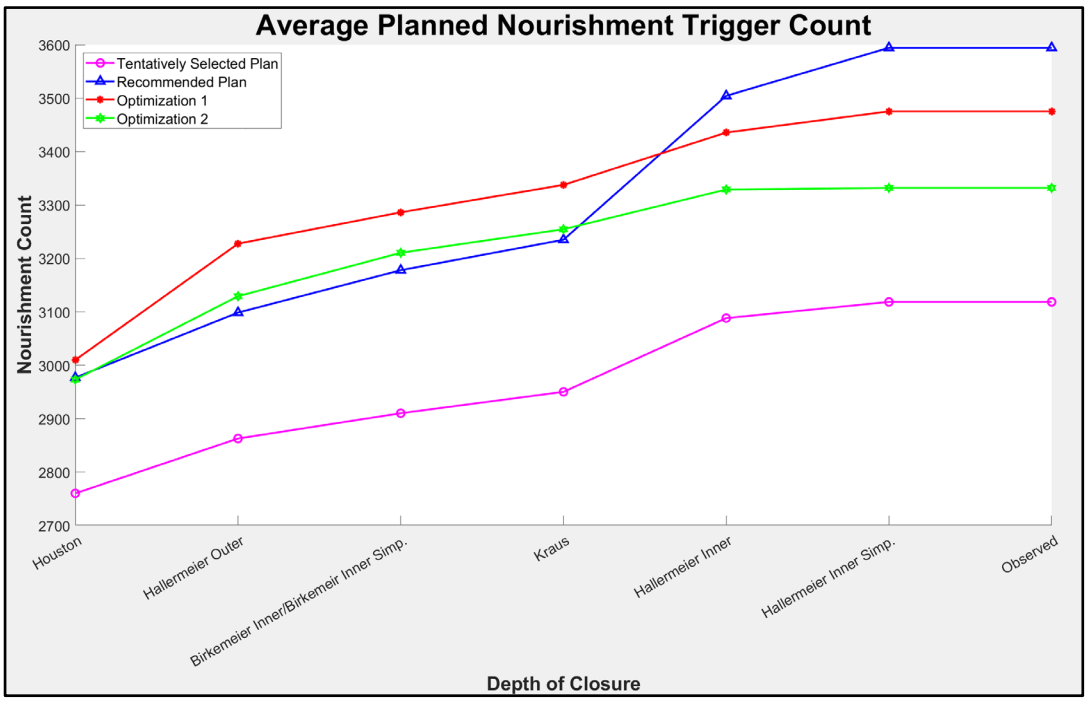

Figure 19: Beach-*fx* Nourishment Trigger Count Results

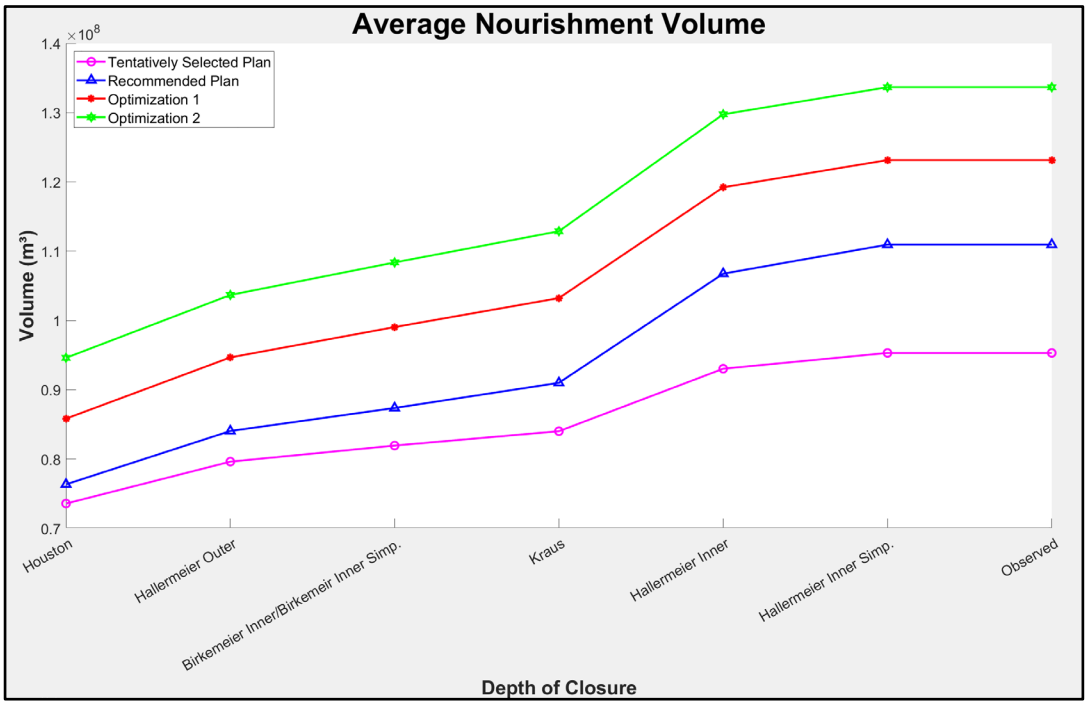

Figure 20: Beach-*fx* Nourishment Volume Results

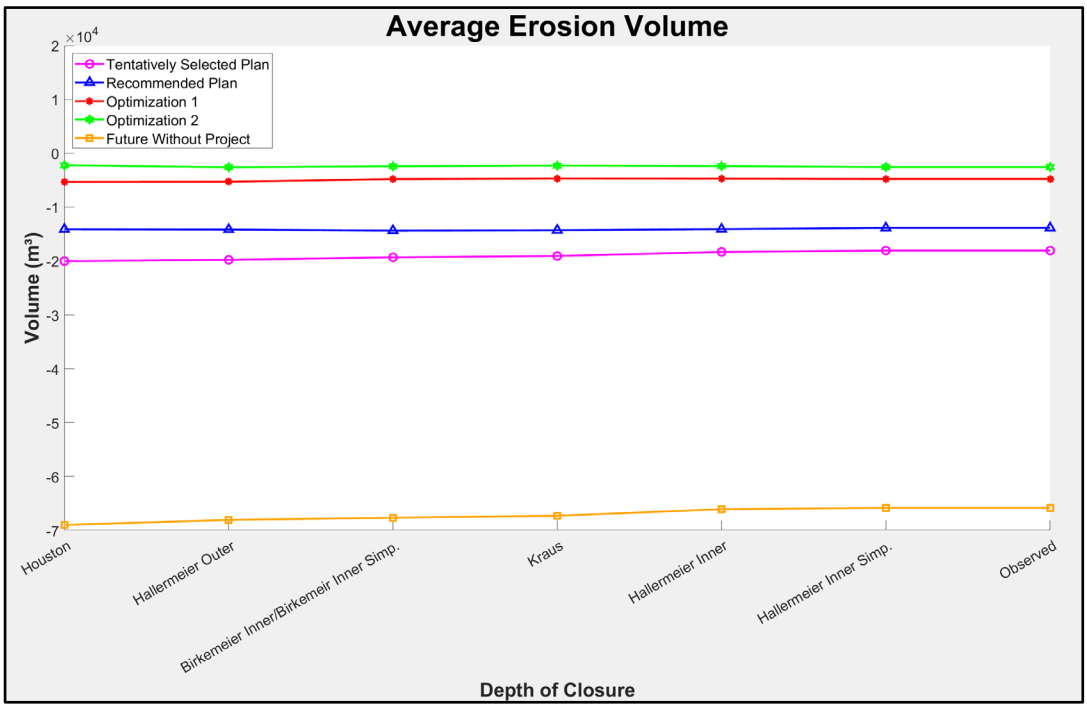

Figure 21: Beach-*fx* Erosion Volume Results

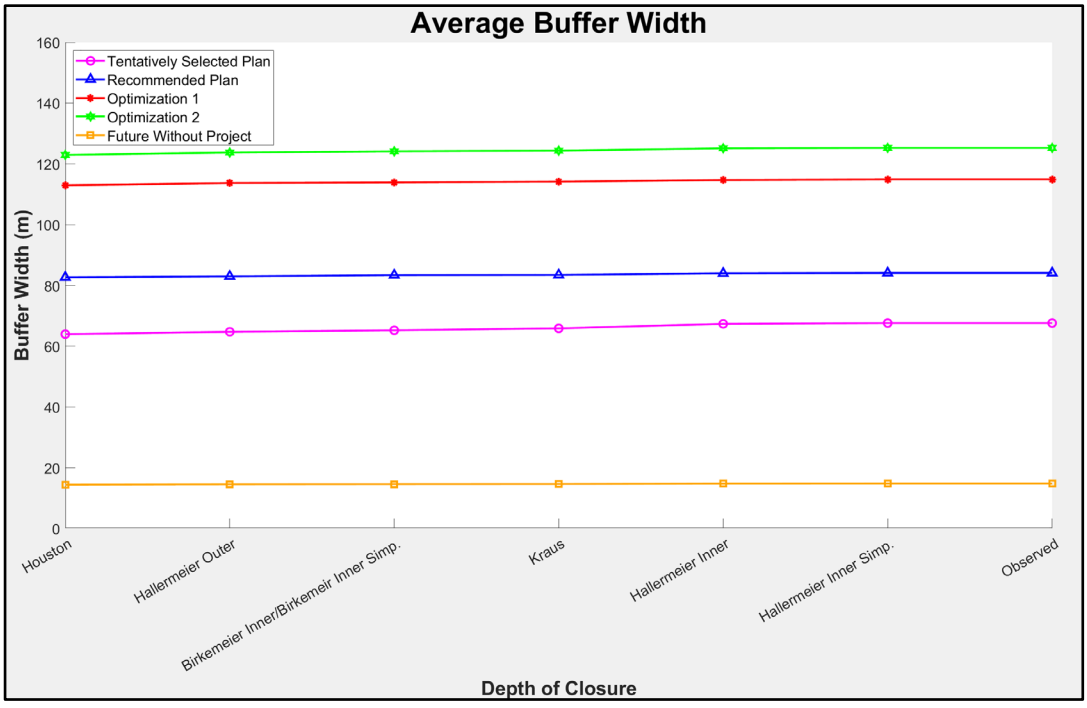

Figure 22: Beach-*fx* Buffer Width Results

The scatter plots provide numerical results on how Beach-*fx* morphology change outputs are impacted by the DOC. In Figures 19 and 20 it is clear that the greater DOC values for Hallermeier Inner, Hallermeier Inner Simplified, and the observed DOC resulted in higher nourishment counts and nourishment volumes for each nourishment plan for the 50 year model life. The majority of nourishment plans experienced an increase in nourishment count or volume at the same rate as the other nourishment plans. However, Hallermeier Inner, Hallermeier Inner Simplified, and the observed DOC caused the recommended nourishment plan to surpass the nourishment counts of the optimization one and optimization two nourishment plans. Figures 21 and 22 show constant values for the total erosion volume and buffer width. Figures 23, 24, 25, and 26 display the percent change of the analysis metric for each scenario where the baseline is the observed DOC.

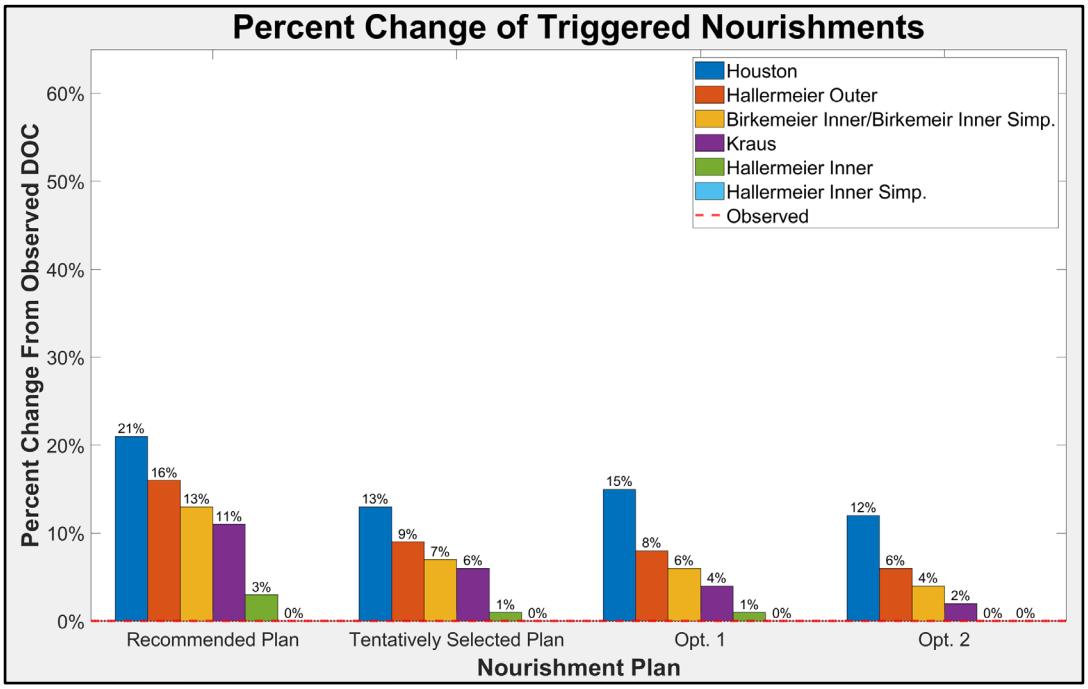

Figure 23: Beach-*fx* Percent Change of Triggered Nourishment Results

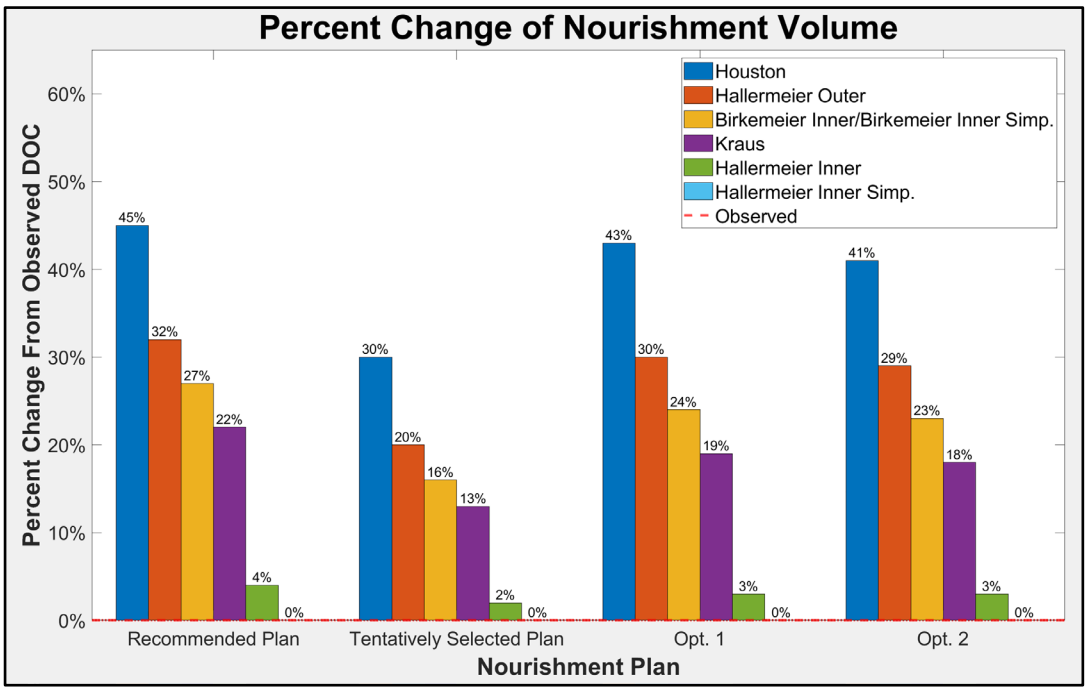

Figure 24: Beach-*fx* Percent Change of Total Nourishment Volume Results

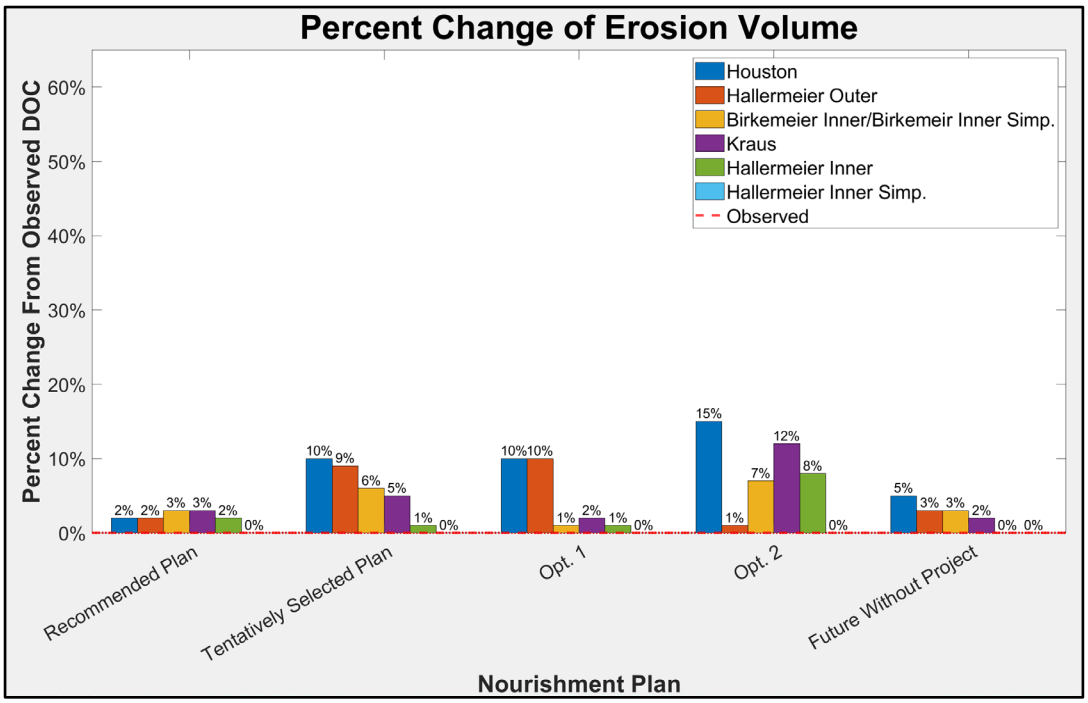

Figure 25: Figure 25: Beach-*fx* Percent Change of Total Erosion Volume Results

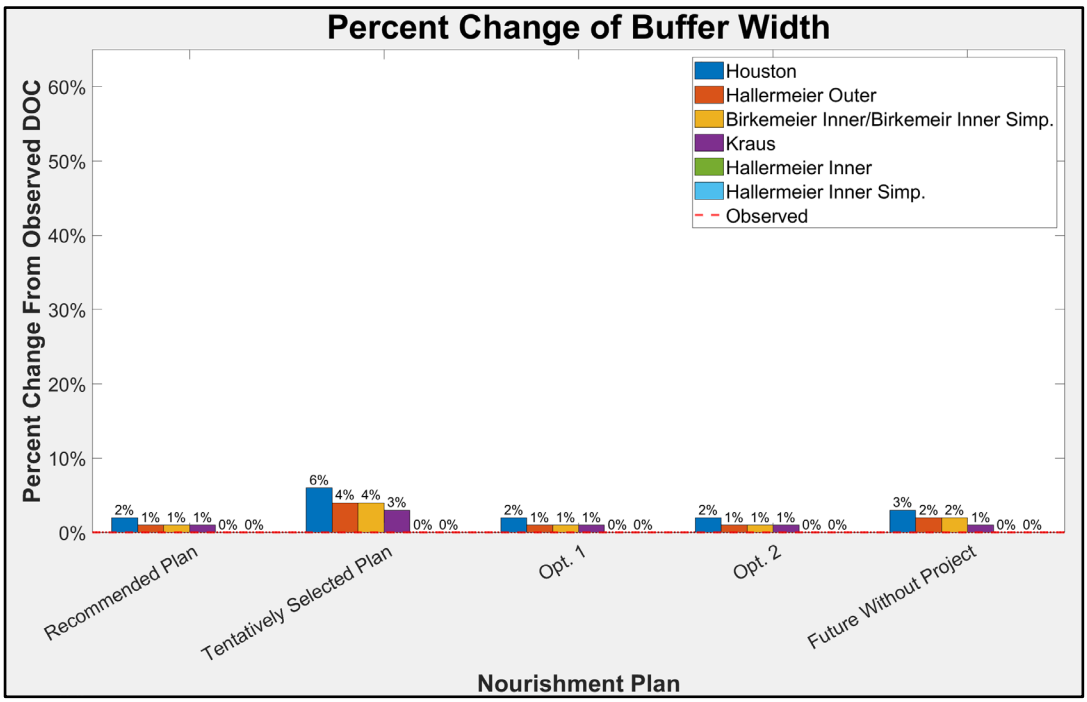

Figure 26: Beach-*fx* Percent Change of Buffer Width Results

6.4 Study Objective 2 Discussion

The morphology change analysis demonstrated that Beach-*fx* has a quantifiable sensitivity to the DOC. For the four morphology change analysis metrics, each nourishment scenario had a similar behavior to the varying DOC values. Houston (1995) consistently had the greatest percent change from the observed DOC ranging from 2% to 45%, followed by Hallermeier Outer (1981), Birkemeier and Birkemeir Simplified (1985), Kraus (1999), and Hallermeier Inner (1978), and finally Hallermeier Inner Simplified (1981). The percent change of total erosion volume showed variability in the percent change from the observed DOC between the different nourishment scenarios. However, Houston (1995) still had the most instances of having the greatest percent change from the observed DOC and Hallermeier Inner had the most instances of having the lowest percent change from the observed DOC.

The percent change of BW and total erosion volume had a low and fair sensitivity to the DOC, indicated by the range of percent change from the observed DOC. The DOC plays a role in various factors impacting the BW such as erosion volume. The DOC is a direct input to the erosion volume calculation through one-line theory using the erosion

volume associated with the CSHORE looked-up response profile. All erosion is applied directly to the dry profile elements, above NAVD88, starting with the dune elevation, and following with the dune width, berm width, and upland width. The BW is a metric of resilience of the dune and beach through a nourishment life and only considers the portion of the profile that can be nourished. The Beach-*fx* modeling scheme included a 90% berm width recovery factor over 21 days that prevents drastic deterioration of the profile and maintains a gradually decreasing BW over time impacting the low percent changes and variability in both the BW and erosion volume metrics. The BW had a sensitivity range of 2-6% for Houston (1995), and a 0% sensitivity for Hallermeier Inner (1978). The total erosion volume had a sensitivity range of 2-15% for Houston (1995), and a range of 0-8% for Hallermeier (1978).

The triggered nourishments and total nourishment volume had the highest sensitivity to the DOC, indicated by the significant percent change from the observed DOC. Each nourishment scenario had the same specifications to trigger a planned nourishment. Once a planned nourishment is triggered the nourishment volume is determined to fill the planned nourishment dimensions from the edge of the berm to the DOC. Further, the more nourishments are triggered the greater the resulting nourishment volume. The number of triggered nourishments had a sensitivity range of 12-21% for Houston (1995), and a ranging sensitivity from 0-3% for Hallermeier Inner (1978). The total erosion volume had a ranging sensitivity from 2-15% for Houston (1995), and a ranging sensitivity from 0-8% for Hallermeier Inner (1978).

Chapter 7

Model Performance

Performance analysis methods help understand the accuracy and biases of morphodynamic models. The brier skill score (BSS) and model bias are methods to measure the model performance. The BSS [17] compares the RMSE in modeled bed level change to the variance of the observed bed level change from the LiDAR survey where z_b is the bed level, Δz_{bLiDAR} (equal to 0.1) is the error of measured bed level, and $\langle\ \rangle$ is an averaging procedure over time series. The BSS is ranked based on the range of qualifications where excellent ranges [1.0 – 0.8], good ranges [0.8 – 0.6], reasonable ranges [0.6 – 0.3], poor ranges [0.3 – 0], and bad < 0 (van Rijn, 2003). The model bias [18] calculates the mean error in the simulation to determine trends in the model errors where dz is the change in pre and post storm profile bed elevation. A model bias greater than one indicates the model is overpredicting bed level change, while a bias less than one indicates the model is underpredicting bed level change.

$$BSS = 1 - \left[\frac{\langle(|z_{bModel,i} - z_{bLiDAR,i}| - \Delta z_{bLiDAR})^2\rangle}{\langle(z_{bLiDAR,initial} - z_{bModel,i})\rangle}\right] \quad [17]$$

$$Bias = \frac{1}{N}\sum_{i=1}^{N}(dz_{b_{LiDAR,i}} - dz_{b_{Model,i}}) \quad [18]$$

7.1 CSHORE & Beach-*fx* Performance Results

The CSHORE BSS was computed with the three profile configurations modeled including the average, trapezoidal representative profile with the average bathymetry appended below datum, and trapezoidal profile with the equilibrium profile appended below datum. Figures 27 and 28 provide a graphical display of the CSHORE BSS and model bias.

Each box plot includes the three model reaches for each post storm event, resulting in six profiles for each box plot.

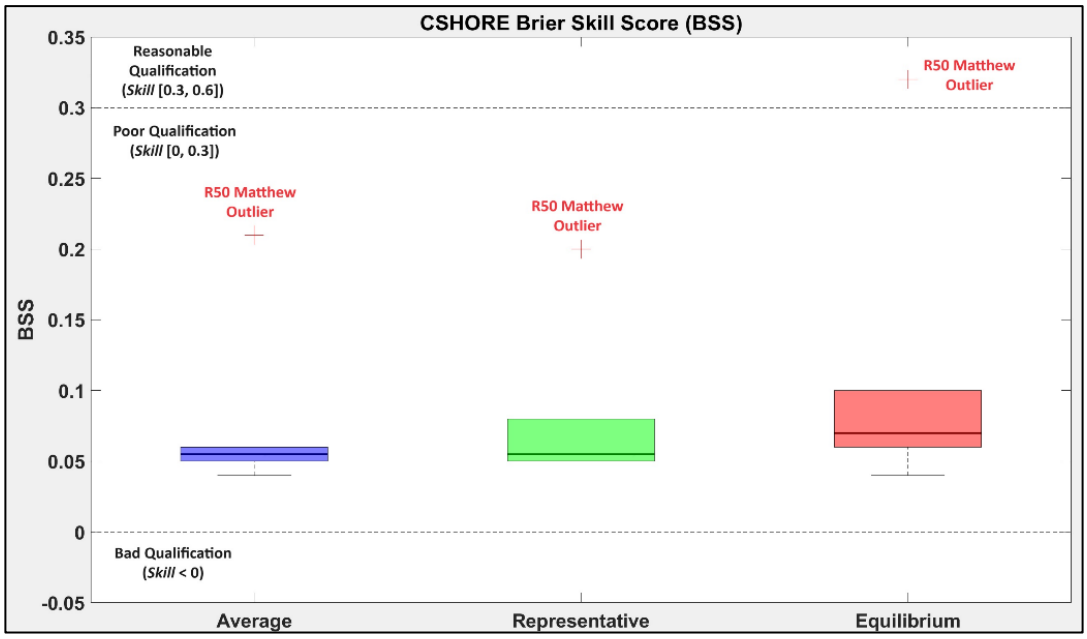

Figure 27: CSHORE BSS Results

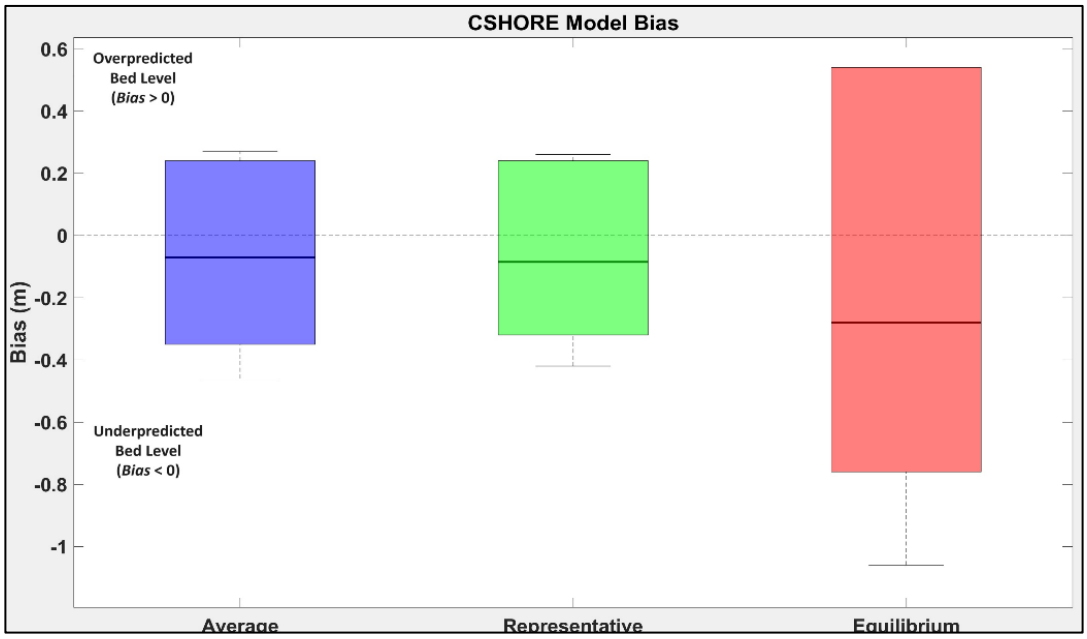

Figure 28: CSHORE Bias Results

CSHORE median BSS falls in the poor qualification range for the majority of profile configurations besides and outlier identified for the model reach R50 Hurricane Matthew. The outlier was identified as being greater than the third quartile plus three times the interquartile range. An analysis of the pre- and post-storm profiles for R50 Hurricane Matthew indicates little profile change. This is consistent with the R50 Hurricane Matthew results when comparing the post-storm LiDAR and CSHORE modeled profiles in Table 7. The CSHORE bias median is less than one across the board indicating an underpredicted bed level for the three profile configurations modeled in CSHORE.

Specific storms and their arrival times can be specified in Beach-*fx* using the specific storm window. The maximum extratropical storm per season was set to zero and the maximum tropical storm was set to one to ensure both hurricanes Matthew and Irma would occur at their respective time stamps in the model. The recovery stage of the profile was selected for extraction of the trapezoidal representative profile from the morphology outputs. The Beach-*fx* BSS and model bias were computed by comparing the trapezoidal representative profiles constructed from the LiDAR survey and compared with the modeled post storm profiles for Hurricane Matthew and Irma. Unlike CSHORE, Beach-*fx* does not model changes to the profile below datum restricting this analysis to only compare the trapezoidal representative profiles above datum. Each box plot includes the three model

reaches. Figures 29 and 30 provide a graphical representation of the Beach-*fx* BSS and model bias.

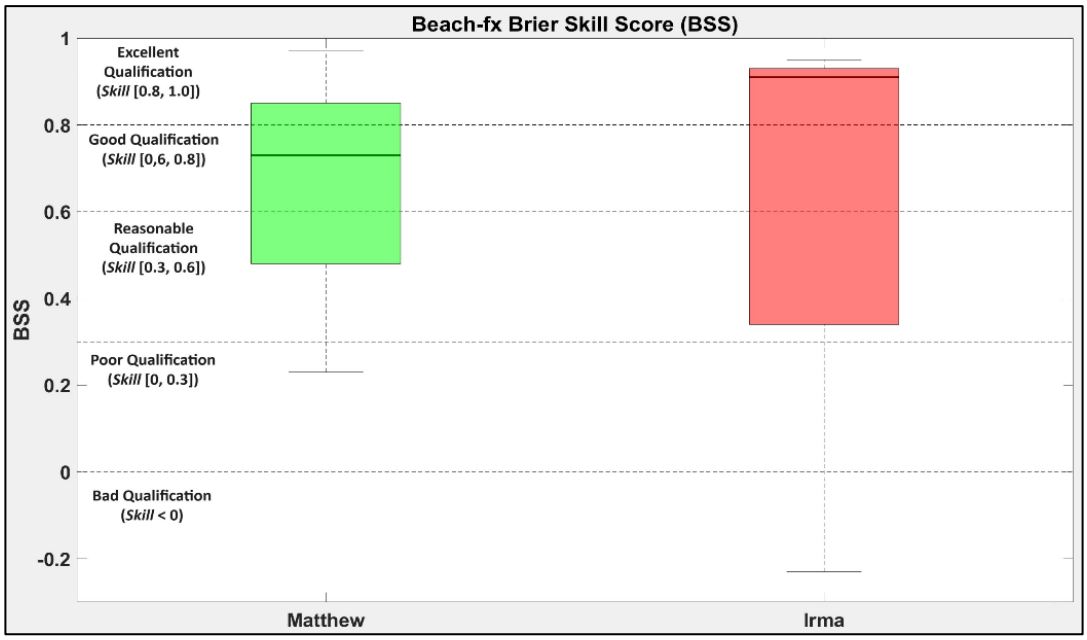

Figure 29: Beach-*fx* BSS Results

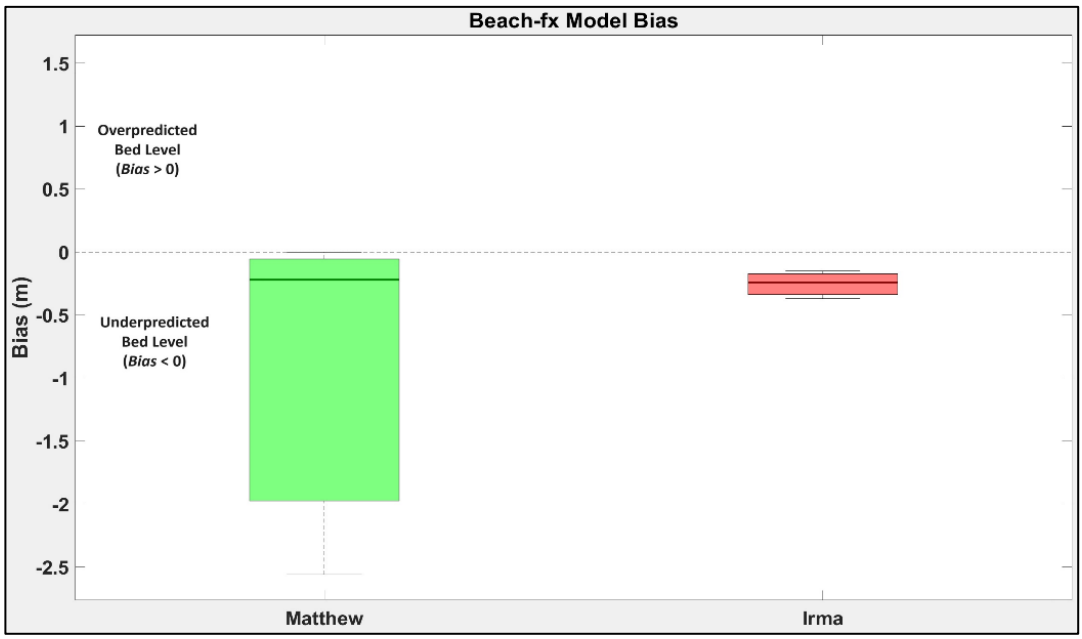

Figure 30: Beach-*fx* Bias Results

Beach-*fx* BSS has a varying range with instances from bad to excellent. The medians fall in the good and excellent qualification ranges. Similarly to CSHORE, the Beach-*fx* bias median is less than one across the board indicating a slight underpredicted bed level for hurricanes Matthew and Irma. The CSHORE and Beach-*fx* model performance methodologies vary significantly, and their results should not be compared.

7.2 Study Objective 3 Discussion

CSHORE and Beach-*fx* both have high computation efficiency when compared to other 2D and 3D morphodynamic models that require supercomputers and high computation times to complete studies. The high computational efficiency comes at the cost of making high level assumptions of beach morphology processes with regards to physics parameterization. Models make assumptions that allow them to be highly useful tools when used correctly and during the right phases of a project. CSHORE and Beach-*fx* play critical roles in beach nourishment planning for the USACE, where the purpose of probabilistic life-cycle scheme in the planning phase is to consider a wide range of nourishment scenarios and the storm damage they reduce. Projects often require a more in-depth modeling scheme during the design phase which may include 2D or 3D morphodynamic models. The CSHORE BSS results faired within the range of values found by Kalligeris et al., (2020) for a study in southern California. The CSHORE bias was slightly lower than the range of values found by Harter and Figlus (2017) for a Texas coastal study. The purpose of Beach-*fx* is to model a probabilistic Monte-Carlo life cycle of a beach profile with applied storm events and triggered nourishment scenarios. Beach-*fx* is not necessarily intended to compare post-storm profiles with LiDAR surveys as the post-storm profiles are provided via the SRD lookup process provided by CSHORE outputs. The bed evolution within Beach-*fx* is therefore a result of the background erosion and storm response profile. Large ranges of BSS observed in Beach-*fx* is not uncommon as seen in by Kalligeris et al., (2020).

Chapter 8

Conclusions

In this study, CSHORE and Beach-*fx* were used to investigate commonly used modeling methods in federal beach nourishment planning. Three FDEP R-monuments representing erosion hotspots at Miami Beach were studied during a period of interest from 2016 through the 2017 hurricane seasons. The CSHORE model predictions were compared to the three profiles constructed from the pre- and post-storm hurricane Matthew and Irma LiDAR surveys. The Beach-*fx* sensitivity to the DOC was tested for six values calculated from empirical formulas and compared to the observed DOC. Finally, model performance was quantified using the BSS and model bias for the profiles modeled and the observed profiles collected from LiDAR surveys.

The representative profile is a valid approximation of the average profile determined by the low RMSE values and by the high R^2 correlations for the full profile and dry profile above NAVD88. The equilibrium profile was a drastic overprediction of the average profile and did not produce meaningful RMSE results when compared to the average profile. The average bathymetry should always be appended to the representative profile below datum to provide higher accuracy compared to the equilibrium profile. This is further supported by the higher R^2 correlation between the average and representative profiles as compared to the average and equilibrium profiles. Statistical analysis should be included in the CSHORE verification process to provide a quantitative analysis that complements the qualitative analysis. Beach-*fx* displayed a varying level of sensitivity to the DOC across the four-morphology metrics measured from output data. Houston (1995) consistently had the greatest percent change from the observed DOC, while Hallermeier Inner and Inner Simplified (1978, 1981) consistently had the lowest percent changes. The number of nourishments triggered, and the nourishment volume exhibited the greatest sensitivities to the DOC. The nourishment volume is a significant cost driver in the calculation of the project BCR used to determine federal recommendations for beach nourishment projects. The results support that empirical DOC calculations can be sufficient in determining a project's DOC using hindcast data. Where feasible, recent observed wave data and bathymetry surveys should be utilized. CSHORE received a poor BSS and consistently underpredicted bed level

change. Beach-*fx* had a varying BSS with the median score between the good and excellent qualifier, and consistently underpredicted bed level change. Performance results varied between CSHORE and Beach-*fx* and should not be compared due to the different analysis methods necessary to extract individual post-storm profiles from Beach-*fx* and due to Beach-*fx* requiring a trapezoidal representative profile and limiting evolution to the profile above datum. This restricted the performance analysis to only allow comparison of the post-storm profiles from Beach-*fx* to the trapezoidal representative profiles above datum from the LiDAR surveys. This study was conducted for a small sample of Miami Beach's coastline at an extremely dynamic hotspot location and from which site-specific conclusions can be drawn for the spatial and temporal area considered. The study conclusions support the hypothesis that the combination of CSHORE and Beach-*fx* is a valid modeling scheme for a probabilistic assessment of coastal storm damage reduction accrued from beach nourishments and can be used with confidence for beach nourishment planning on Miami Beach.

References

Birkemeier, W. A. (1985). Field data on seaward limit of profile change. *Journal of Waterway, Port, Coastal and Ocean Engineering 111*(3):598–602.

Brutsché, K., Rosati, J., Pollock, C., McFall, B. (2016). Coastal Resilience Metrics from Beach-*fx*. *ERDC/CHL CHETN-VI-49*. Vicksburg, MS: US Army Engineer Research and Development Center.

Dean, R., Dalrymple, R. (2001). Coastal Processes with Engineering Application. *Cambridge University Press.*

Durkin, M. and Chambers, K. (2019). Calculating Depth of Closure Using WIS Hindcast Data. ERDC/CHL CHETN-VI-45. Vicksburg, MS: US Army Engineer Research and Development Center.

Florida Department of Environmental Protection (2023). Critically Eroded Beaches in Florida. *Office of Resilience and Coastal Protection*, 6-45.

Gravens, M. B. and Permenter, R. (2022). Beach-*fx* Technical Reference Manual. *ERDC/CHL TR-10-X.* Vicksburg, MS: US Army Engineer Research and Development Center.

Gravens, M. B., R. M. Males, and D. A. Moser (2007). Beach-*fx*: Monte Carlo Life-Cycle Simulation Model for Estimating Shore Protection Project Evolution and Cost bcr Analyses. *Shore and Beach 75*(1): 12–19.

Hallermeier, R. J. (1978). Uses for a calculated limit depth to beach erosion. *Proceedings, Coastal Engineering 1978*:1493–1512.

Hallermeier, R. J. (1981). A profile zonation for seasonal sand beaches from wave climate. *Coastal Eng. 4*:253–277.

Harter, C. and Figlus, J. (2017). Numerical modeling of the morphodynamic response of a low-lying barrier island beach and foredune system inundated during Hurricane Ike using XBeach and CSHORE. Coastal Engineering 120 (2017) 64–74.

Houston, J.R. (1995). Beach-fill volume required to produce specific dry beach width. ERDC/CETN II-32. Vicksburg, MS: US Army Corps of Engineers, Waterways Experiment Station.

Johnson, B.D. and Sanderson, D. (2020). On the Use of CSHORE for Beach-*fx*. ERDC/CHETN-II-59. Vicksburg, MS: US Army Engineer Research and Development Center.

Johnson, B. D., N, Kobayashi and M. B. Gravens (2012). Cross-Shore Numerical Model CSHORE for Waves, Currents, Sediment Transport and Beach Profile Evolution. *ERDC/CHL TR-12-22.* Vicksburg, MS: US Army Engineer Research and Development Center.

Kalligeris, N., Smit, P.B., Ludka, B.C., Guza, R.T., Gallien, T.W. (2020). Calibration and assessment of process-based numerical models for beach profile evolution in southern California. Coastal Engineering, Volume 158,103650,

Kalnay, E., Kanamitsu, M., Kistler, R., Collins, W., Deaven, D., Gandin, L., Iredell, M., Saha, S., White, G., Woollen, J., Zhu, Y., Chelliah, M., Ebisuzaki, W., Higgins, W., Janowiak, J., Mo, K., Ropelewski, C., Wang, J., Leetmaa, A., Reynolds, R., Jenne, R., and Joseph, D. (1996) The NCEP/NCAR 40-Year Reanalysis Project. Bulletin of the American Meteorological Society,77,437-471.

Kraus, N. and Galgano, F (2001). Beach Erosional Hot Spots: Types, Causes and Solutions. *ERDC/CHL CHETN-II-44*. Vicksburg, MS: US Army Engineer Research and Development Center.

Kobayashi, N., de los Santos, F., and Kearney, P. (2008). Time-Averaged Probabilistic Model for Irregular Wave Runup on Permeable Slopes.

Kobayashi, N., Buck, M., Payo, M., Johnson B.D. (2009). Berm and Dune Erosion During a Storm. *J. Waterw. Port. Coast. Ocean Eng., 135 (1)*, pp. 1-10).

Lin, P. and Sasso, R.H. (1996). Influence of Nearshore Hardbottom on Regional Sediment Transport. *International Conference on Coastal Engineering*, *CONFERENCE PROCEEDINGS NO. 25.*

National Oceanographic and Atmospheric Administration Historical Hurricane Tracks (2022a). Hurricane Irma and Hurricane Matthew.

National Oceanographic and Atmospheric Administration (2022b). Global and Regional Sea Level Rise Scenarios for the United States. *NOS Technical Report.*

Robertson, W.V., Zhang, K., Finkl, C.W., Whitman, D. (2008). Hydrodynamic and geologic influence of event-dependent depth of closure along the South Florida Atlantic Coast. Marine Geology 252 (2008) 156–165.

Rogers, C.M., Jacobson, K.A., and Gravens, M. (2009). Beach-*fx* User's Maunal: Version 1.0. ERDC/CHL SR-09-6. Vicksburg, MS: US Army Engineer Research and Development Center.

Southeast Florida Regional Climate Change Compact's Sea Level Rise Ad Hoc Work Group (2019). Unified Sea Level Rise Projection Southeast Florida.

Spurgeon, S. (2022). Resilience Metrics at Panama City Beach, Florida. *University of South Alabama ProQuest Dissertations Publishing, 29164039*.

Tolman, H.L. (2014). User Manual and System Documentation of WAVEWATCH III Version 4.18.

US Army Corps of Engineers Headquarters (2001). Historical Vignette 015 -16 March 1802, Establishing the Corps of Engineers. Washington, D.C.

US Army Corps of Engineers Headquarters (2019). ER 1110-2-8162, Sea-level Change Considerations in Civil Works Programs. Washington, D.C.

US Army Corps of Engineers Headquarters (2019). EP 1110-2-1, Procedures to Evaluate Sea-Level Change: Impacts, Response, and Adaption. Washington, D.C.

US Army Corps of Engineers, Jacksonville District (2022). Miami-Dade County Florida, Coastal Storm Risk Management Project, Appendix A: Engineering

US Army Corps of Engineers, Institute for Water Resources (2007). Beach Nourishment How Beach Nourishment Projects Work. *Shore Protection Assessment. Alexandria, VA: US Army Engineer Institute for Water Resources.*

US Census Bureau (2021). Emergency Management Coastal Areas.

US Code, 549a, Supplement 4, Title 33 - NAVIGATION AND NAVIGABLE WATERS.

Van Rinj, L.C., Walstra, D.J.R., Grasmeijer, B., Sutherland, J., Pan, S., Sierra, J.P. (2003). The predictability of cross-shore bed evolution of sandy beaches at the time scale of storms and seasons using process-based Profile models. Coastal Engineering 47 (2003) 295 – 327.

Appendix A: Post Processed ArcGIS Profile Summary

Pre-Hurricane Matthew

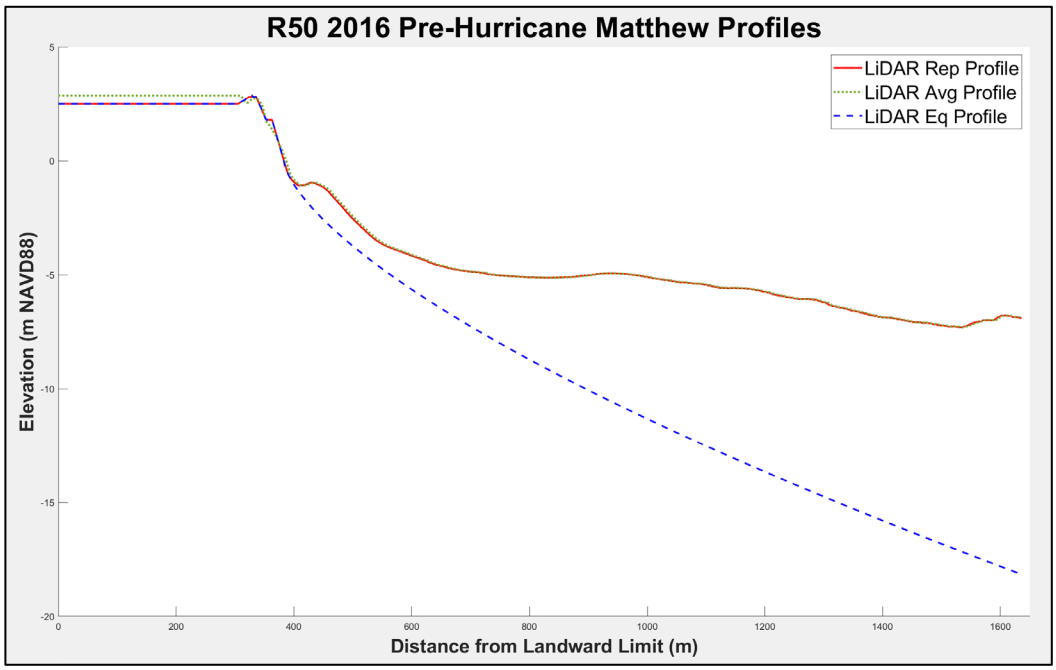

A 1

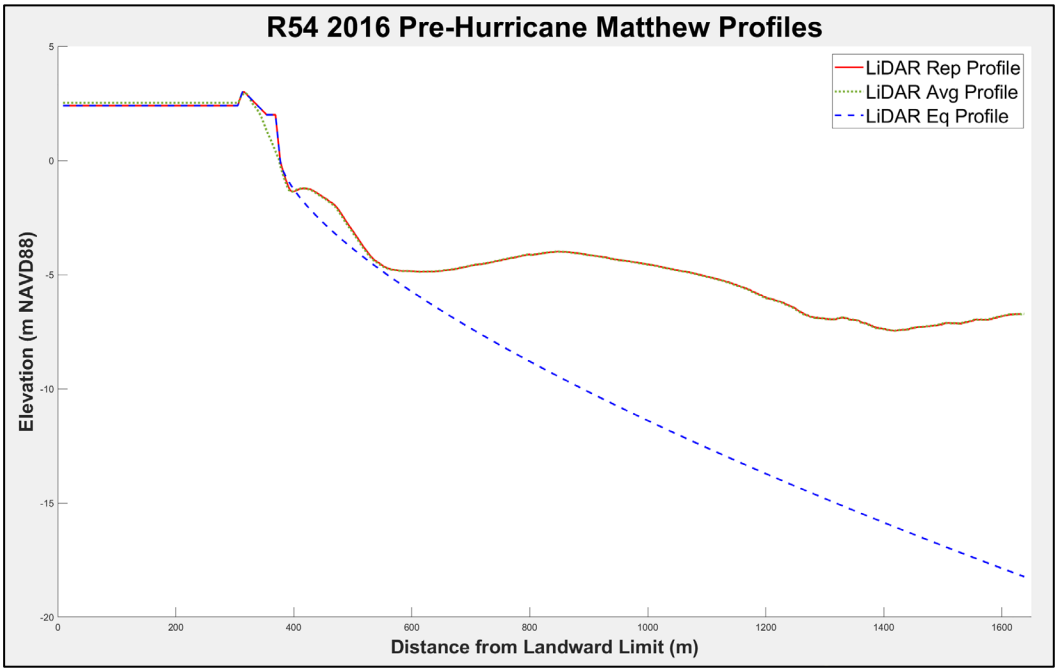

A 2

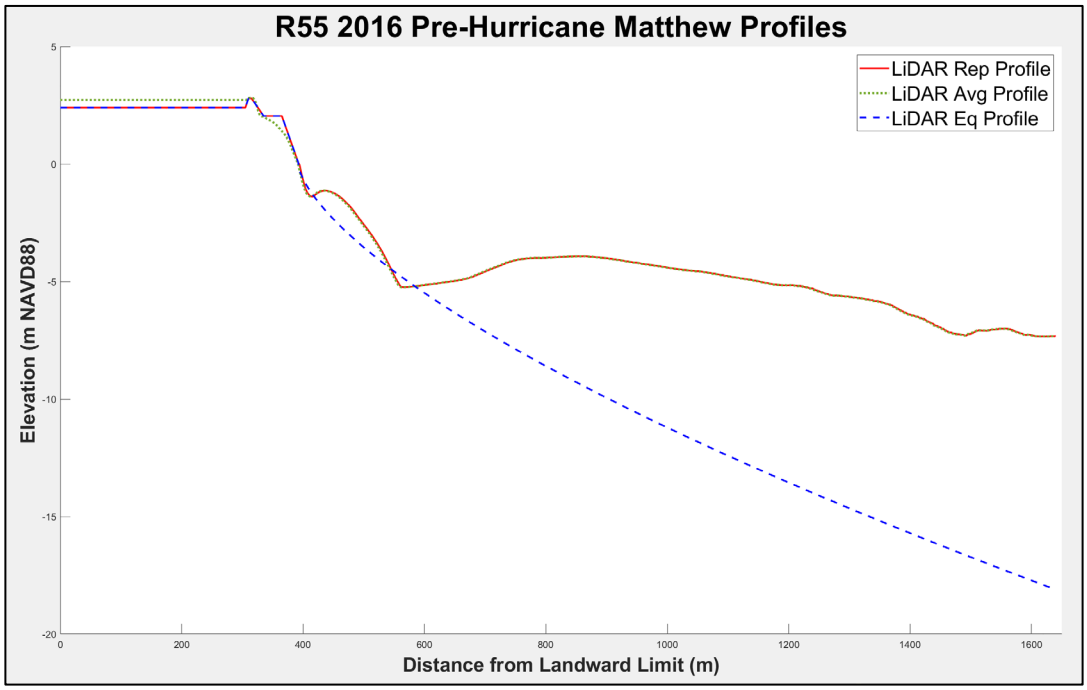

A 3

Post-Hurricane Matthew/Pre-Hurricane Irma

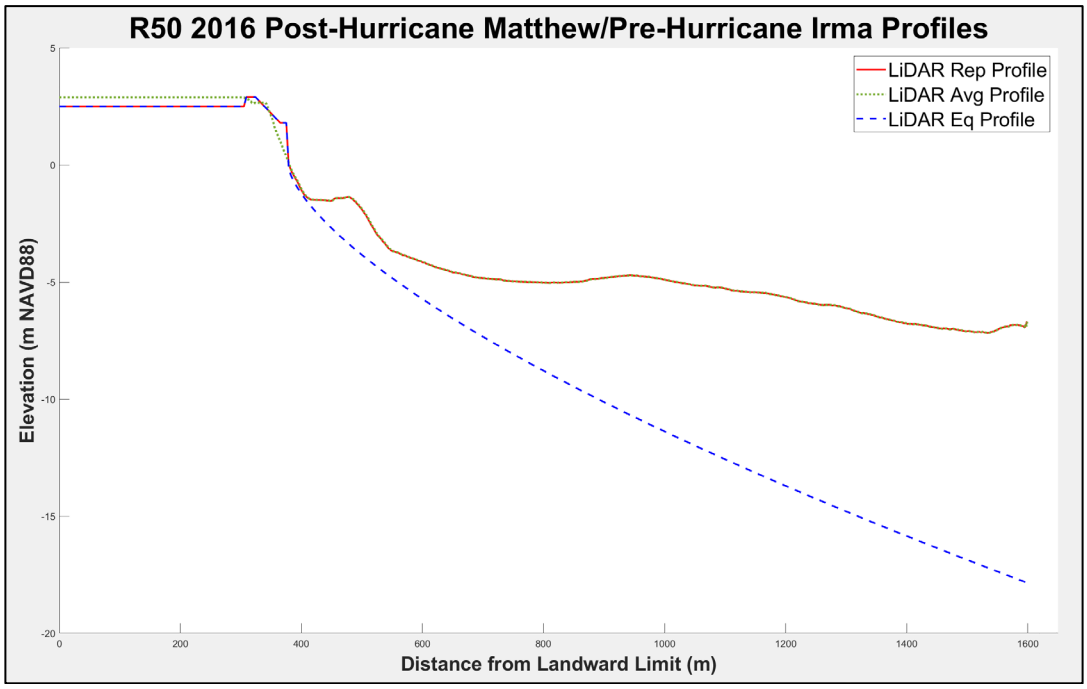

A 4

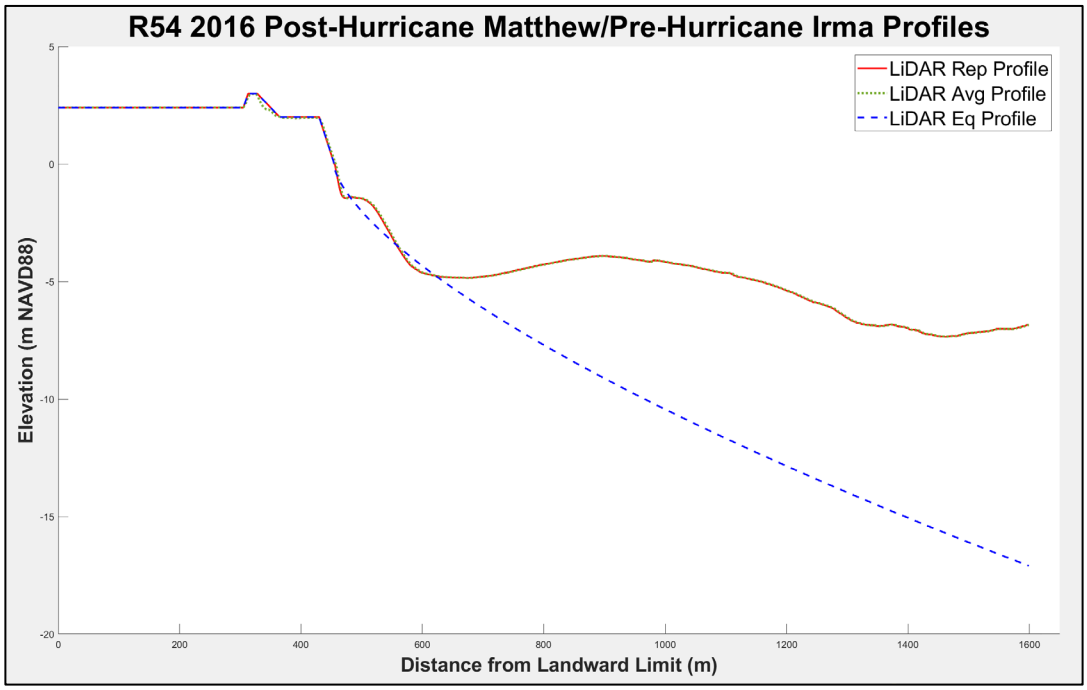
R54 2016 Post-Hurricane Matthew/Pre-Hurricane Irma Profiles
LiDAR Rep Profile
LiDAR Avg Profile
LiDAR Eq Profile
Elevation (m NAVD88)
Distance from Landward Limit (m)
5
0
-5
-10
-15
-20
0
200
400
600
800
1000
1200
1400
1600

A 5

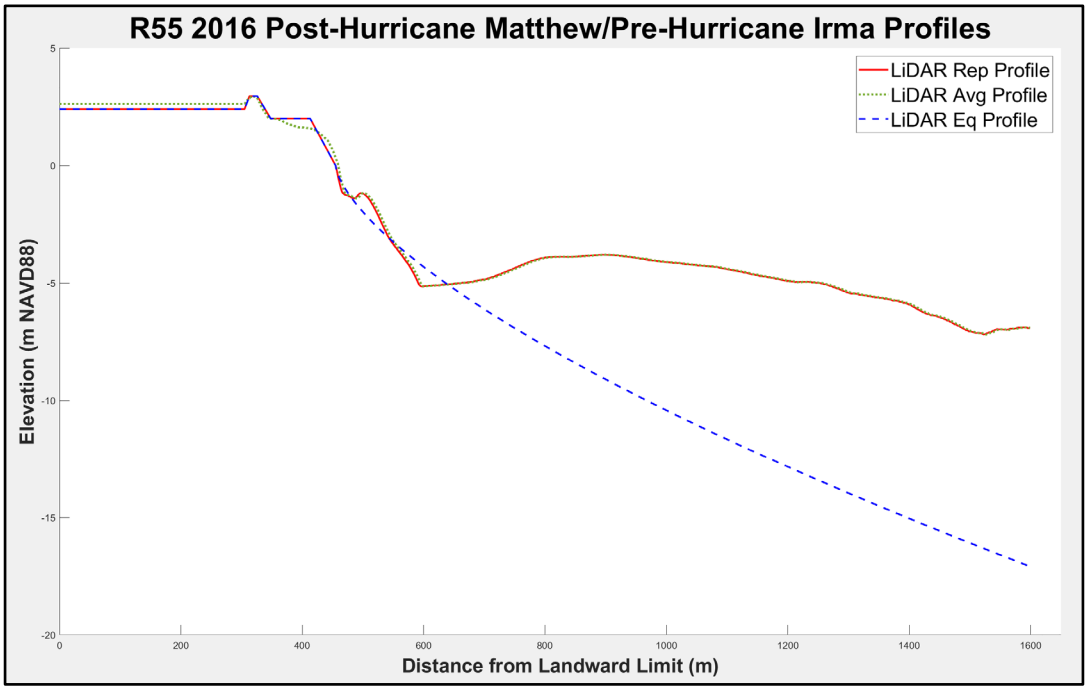
R55 2016 Post-Hurricane Matthew/Pre-Hurricane Irma Profiles
LiDAR Rep Profile
LiDAR Avg Profile
LiDAR Eq Profile
Elevation (m NAVD88)
Distance from Landward Limit (m)
5
0
-5
-10
-15
-20
0
200
400
600
800
1000
1200
1400
1600

A 6

Post-Hurricane Irma

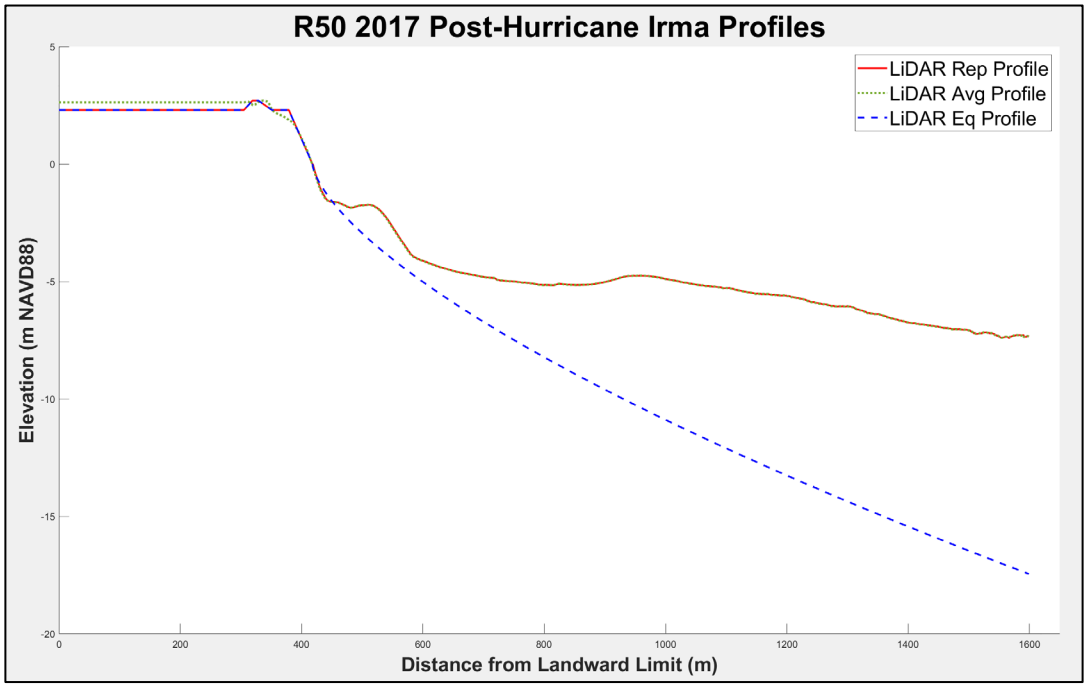

A 7

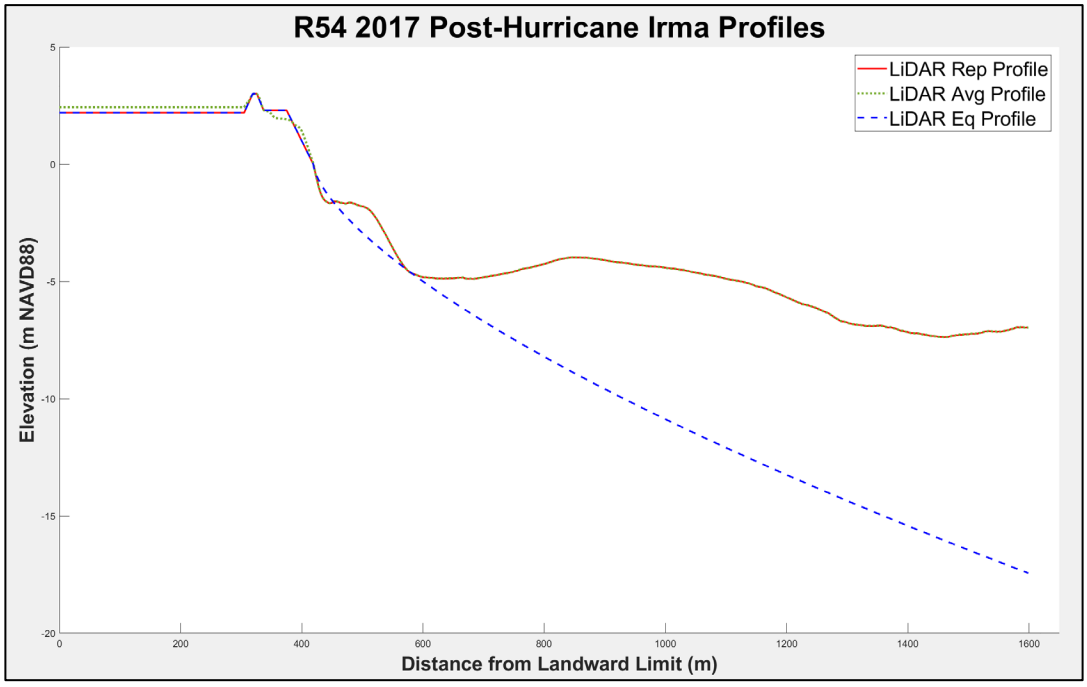

A 8

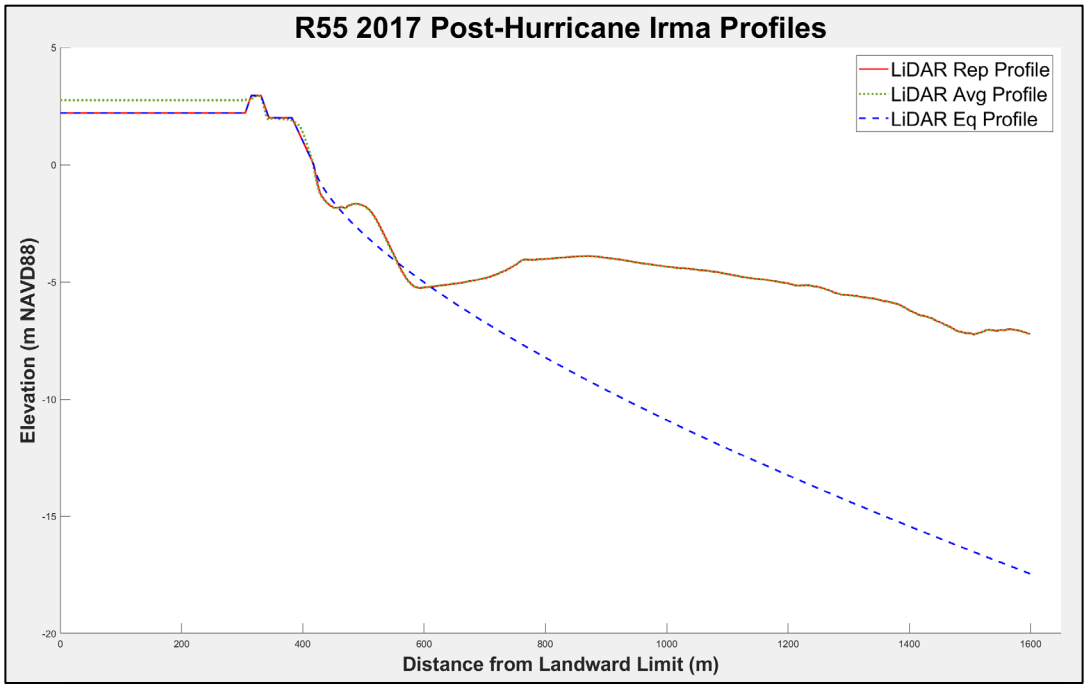
R55 2017 Post-Hurricane Irma Profiles
LiDAR Rep Profile
LiDAR Avg Profile
LiDAR Eq Profile
Elevation (m NAVD88)
Distance from Landward Limit (m)
5
0
-5
-10
-15
-20
0
200
400
600
800
1000
1200
1400
1600

A 9

Appendix B: Modeled Profiles

Hurricane Matthew

Average Profiles

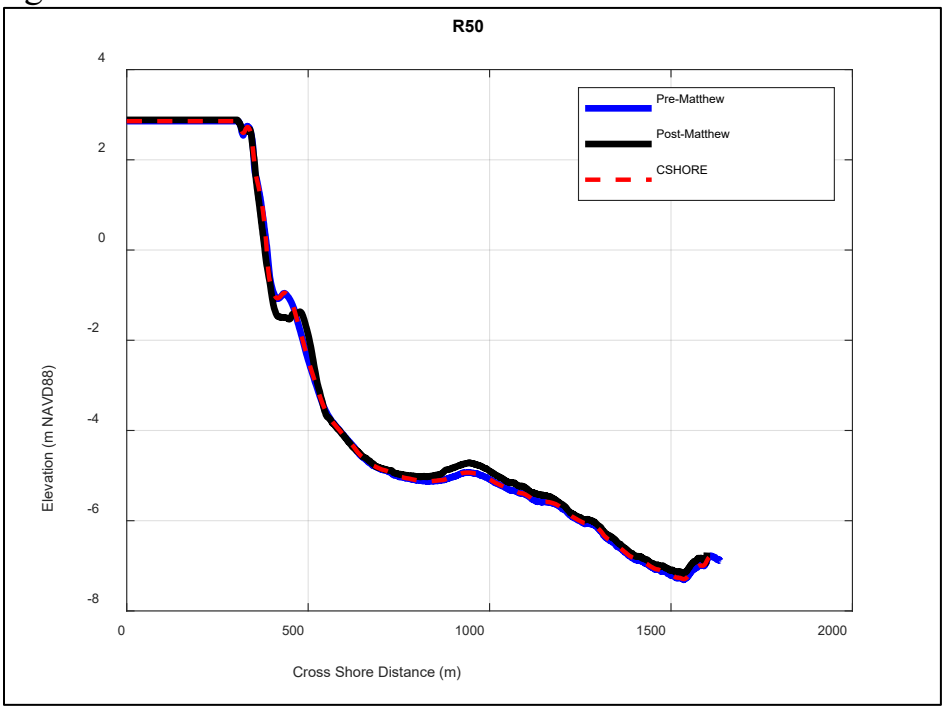

A 10

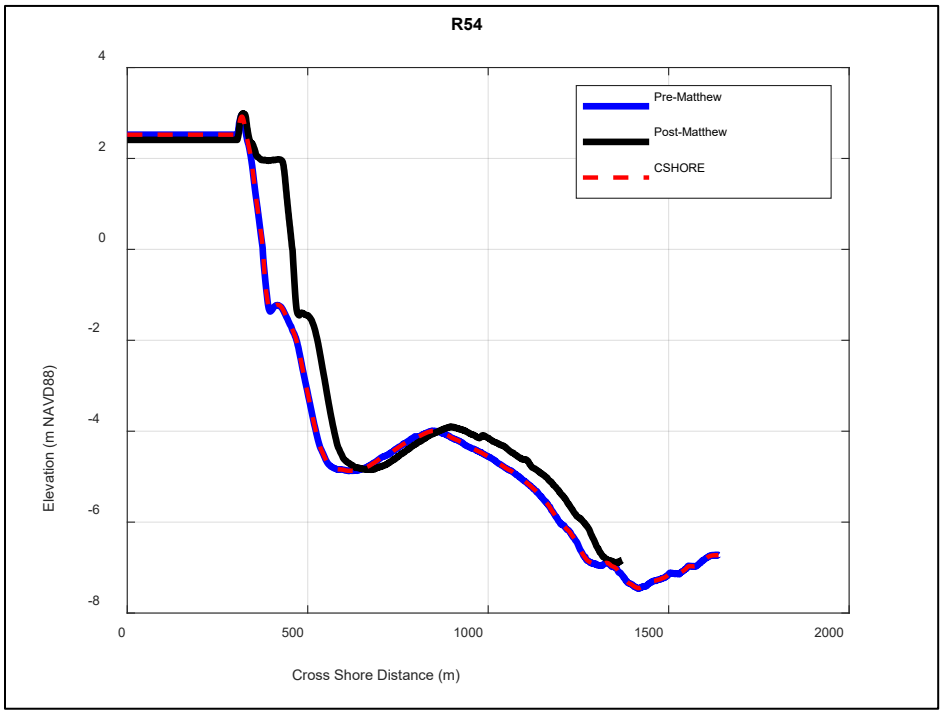
R54
Pre-Matthew
Post-Matthew
CSHORE
Elevation (m NAVD88)
Cross Shore Distance (m)
4
2
0
-2
-4
-6
-8
0
500
1000
1500
2000

A 11

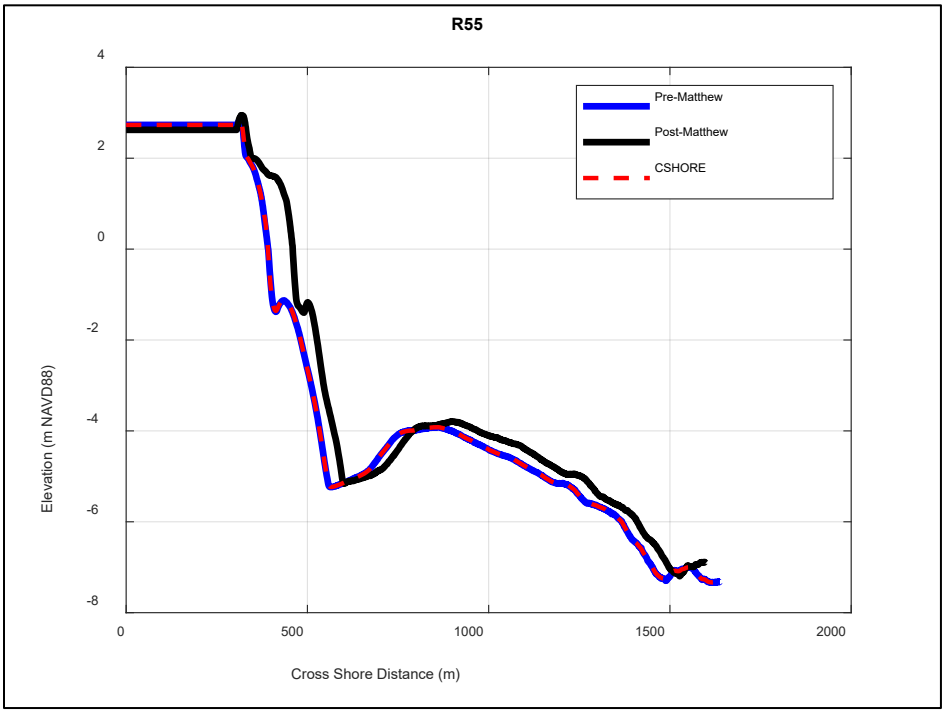
R55
Pre-Matthew
Post-Matthew
CSHORE
Elevation (m NAVD88)
Cross Shore Distance (m)
4
2
0
-2
-4
-6
-8
0
500
1000
1500
2000

A 12

Representative Profiles

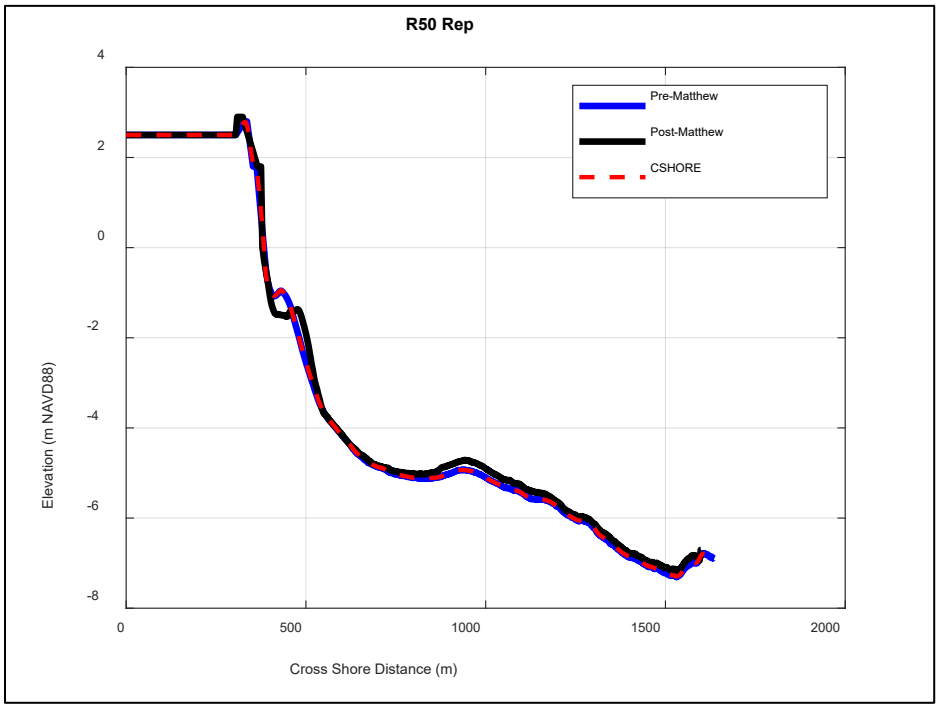

A 13

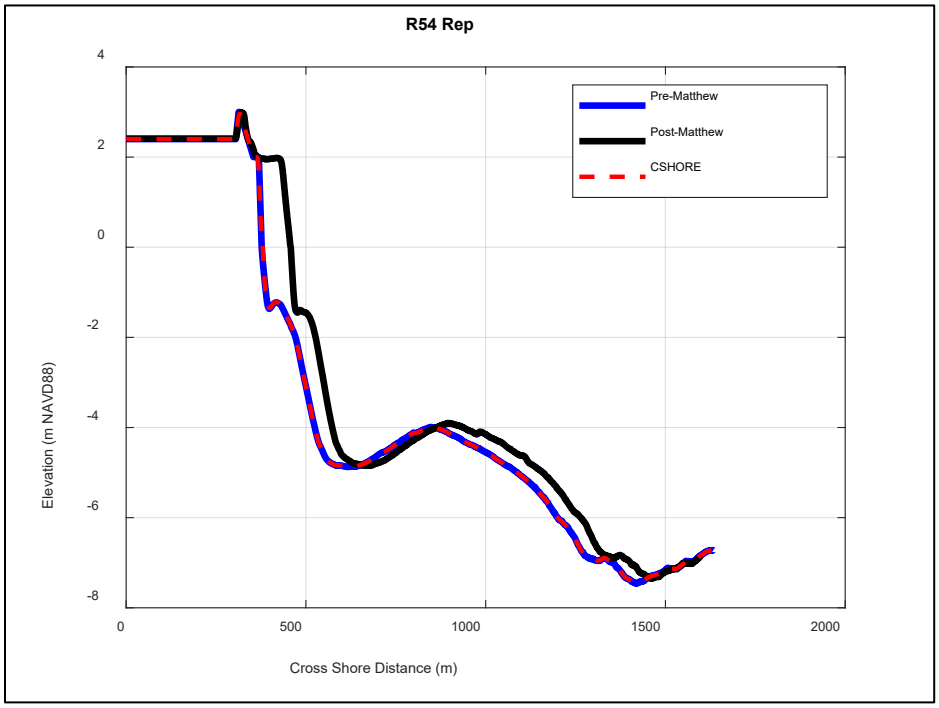

A 14

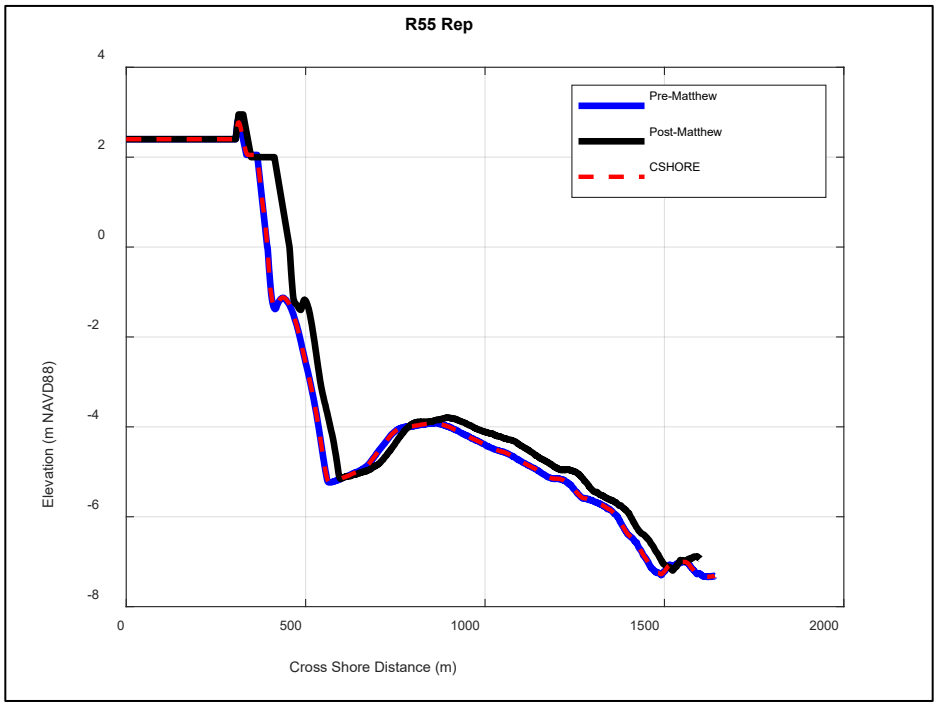

A 15

Equilibrium Profiles

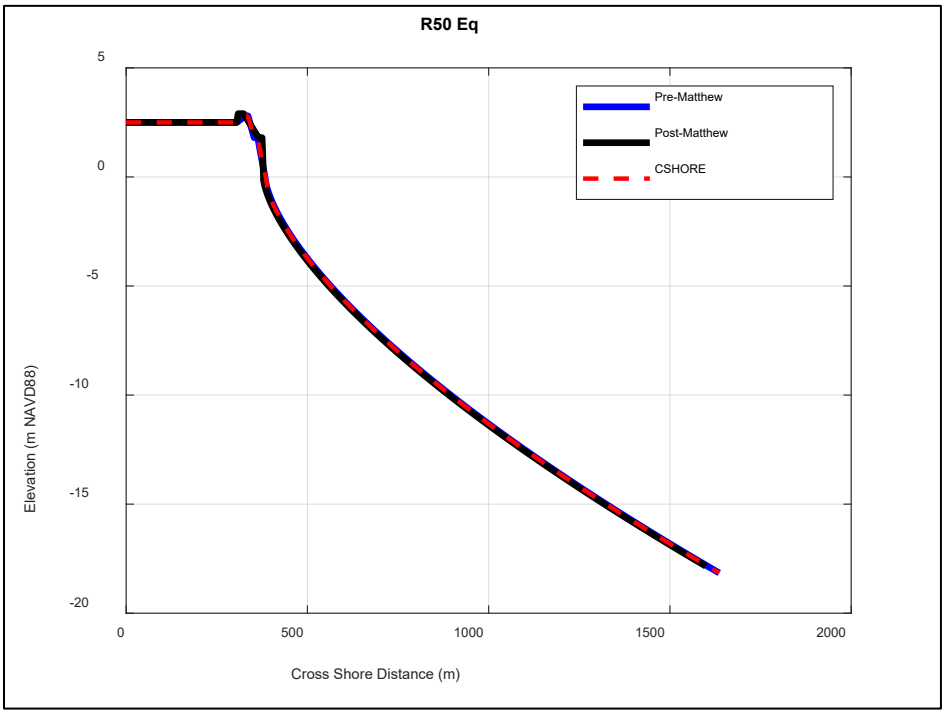

A 16

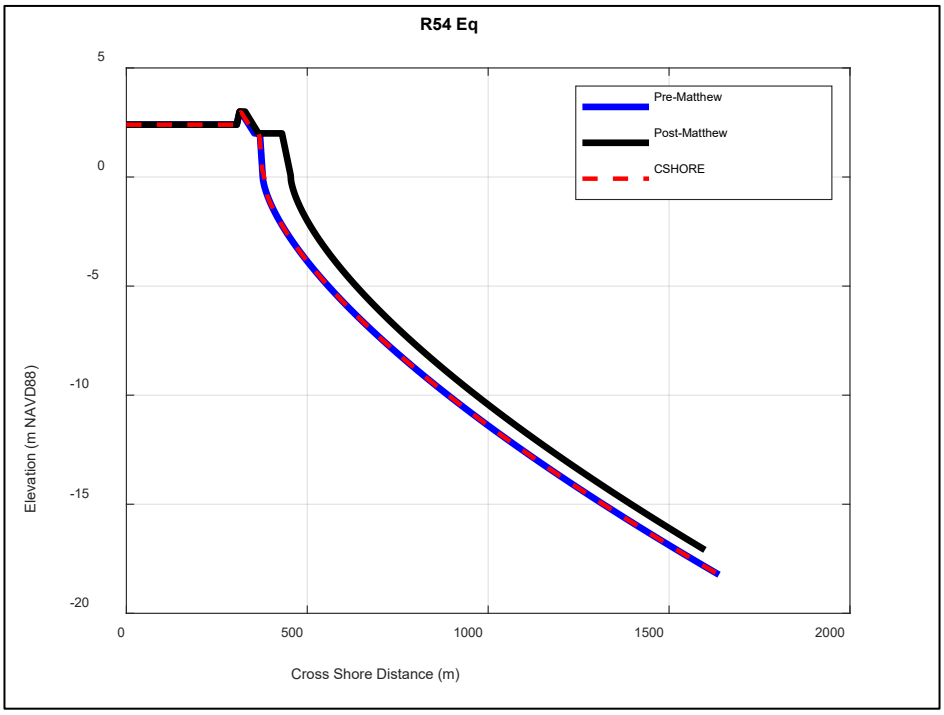
R54 Eq
Pre-Matthew
Post-Matthew
CSHORE
Elevation (m NAVD88)
Cross Shore Distance (m)
5
0
-5
-10
-15
-20
0
500
1000
1500
2000

A 17

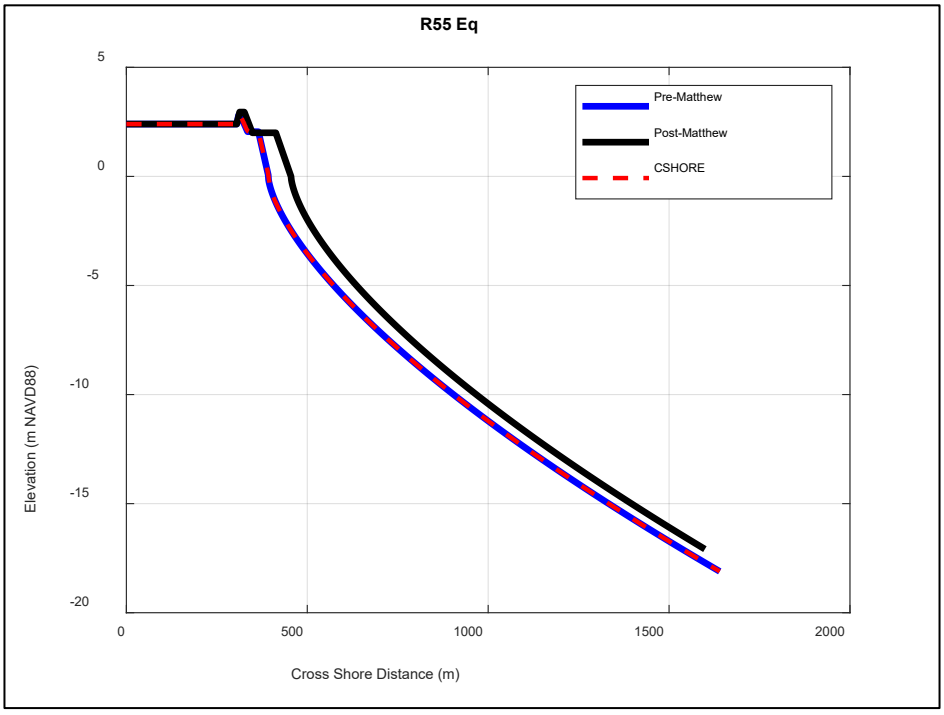
R55 Eq
Pre-Matthew
Post-Matthew
CSHORE
Elevation (m NAVD88)
Cross Shore Distance (m)
5
0
-5
-10
-15
-20
0
500
1000
1500
2000

A 18

Hurricane Irma

Average Profiles

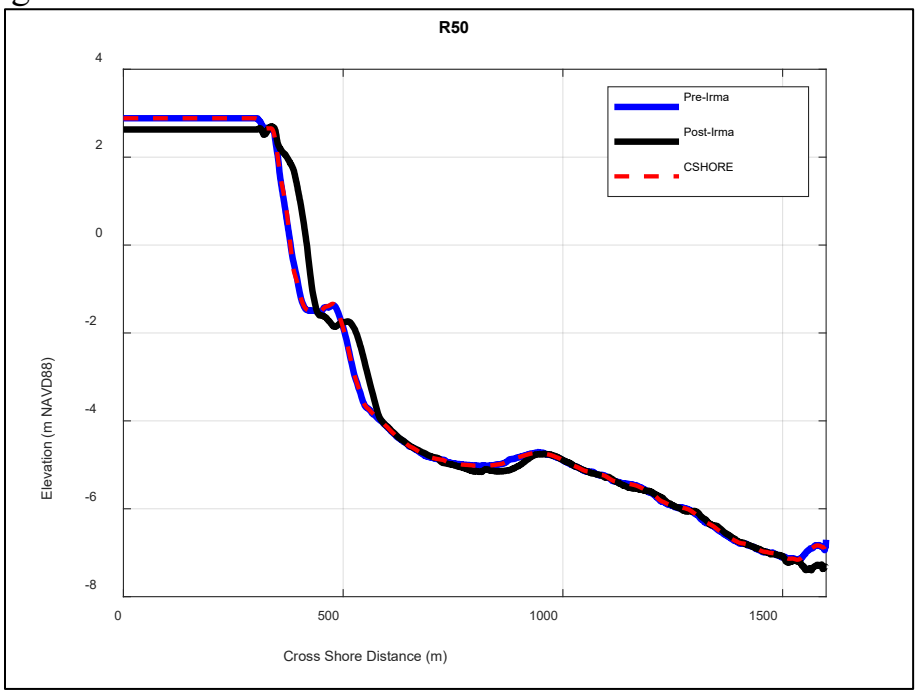

A 19

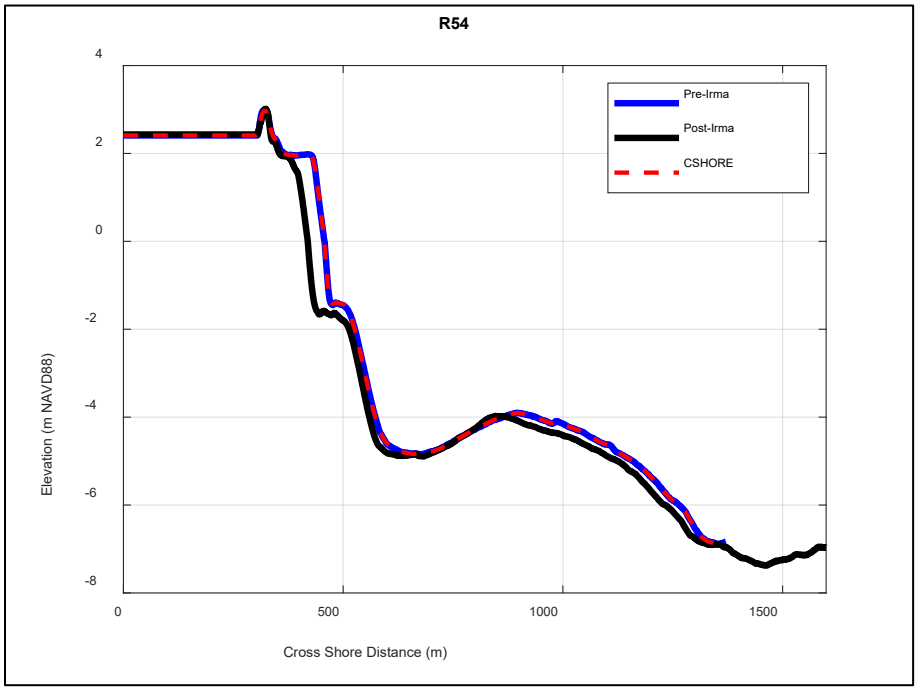
R54
Pre-Irma
Post-Irma
CSHORE
Elevation (m NAVD88)
Cross Shore Distance (m)
4
2
0
-2
-4
-6
-8
0
500
1000
1500

A 20

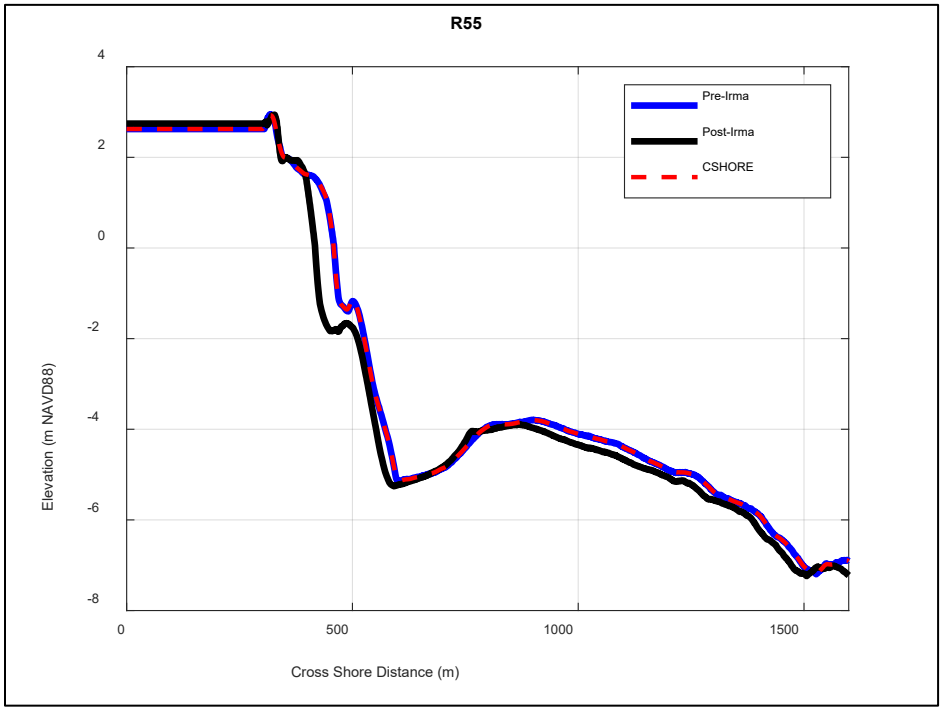
R55
Pre-Irma
Post-Irma
CSHORE
Elevation (m NAVD88)
Cross Shore Distance (m)
4
2
0
-2
-4
-6
-8
0
500
1000
1500

A 21

Representative Profiles

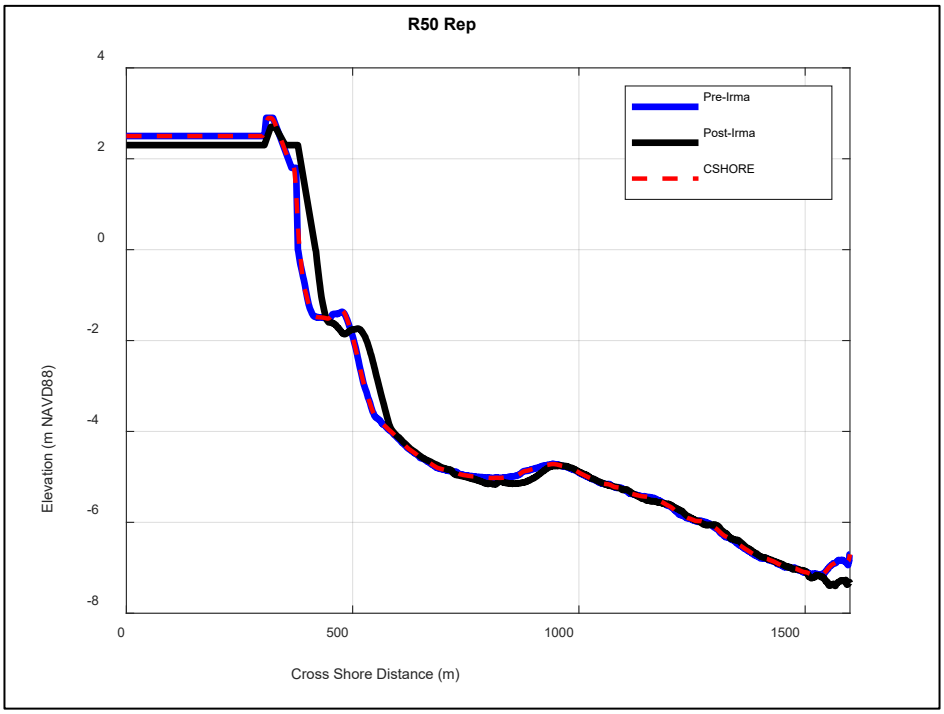

A 22

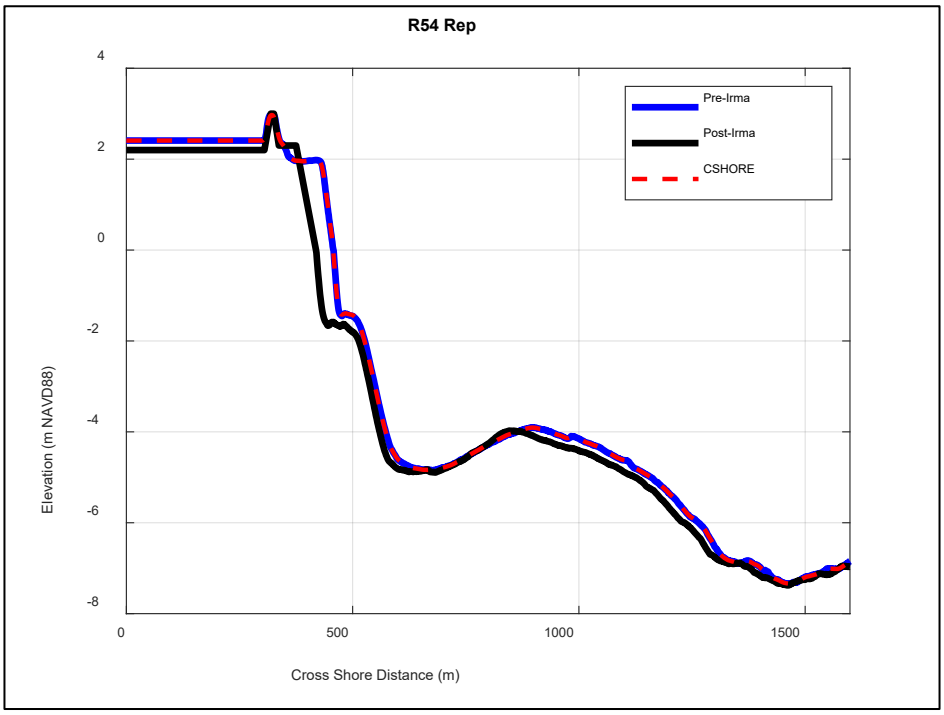

A 23

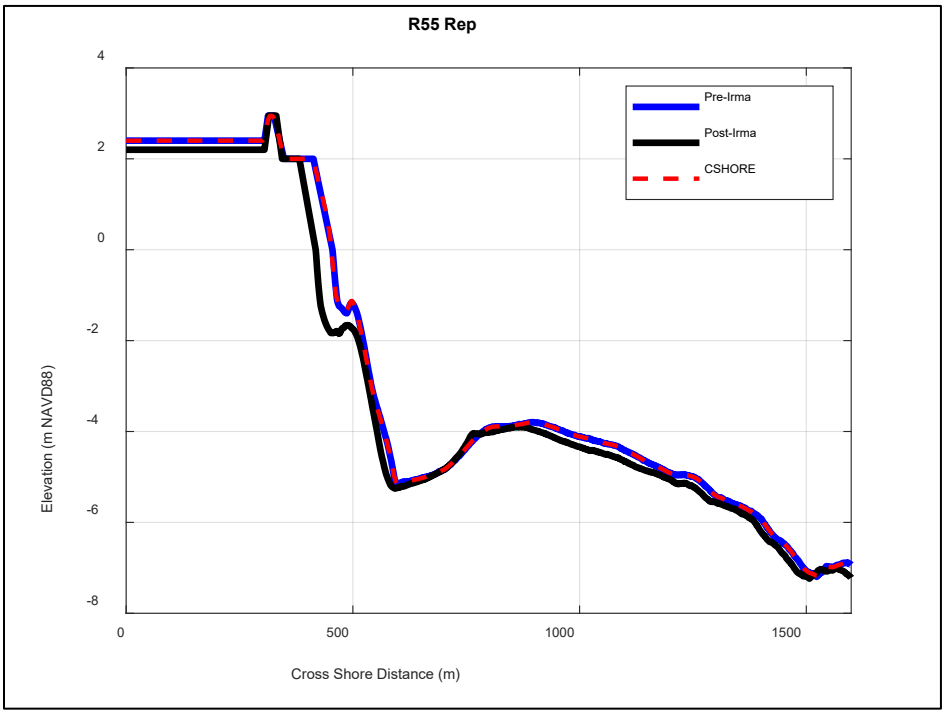
R55 Rep
Pre-Irma
Post-Irma
CSHORE
Elevation (m NAVD88)
Cross Shore Distance (m)
4
2
0
-2
-4
-6
-8
0
500
1000
1500

A 24

Equilibrium Profiles

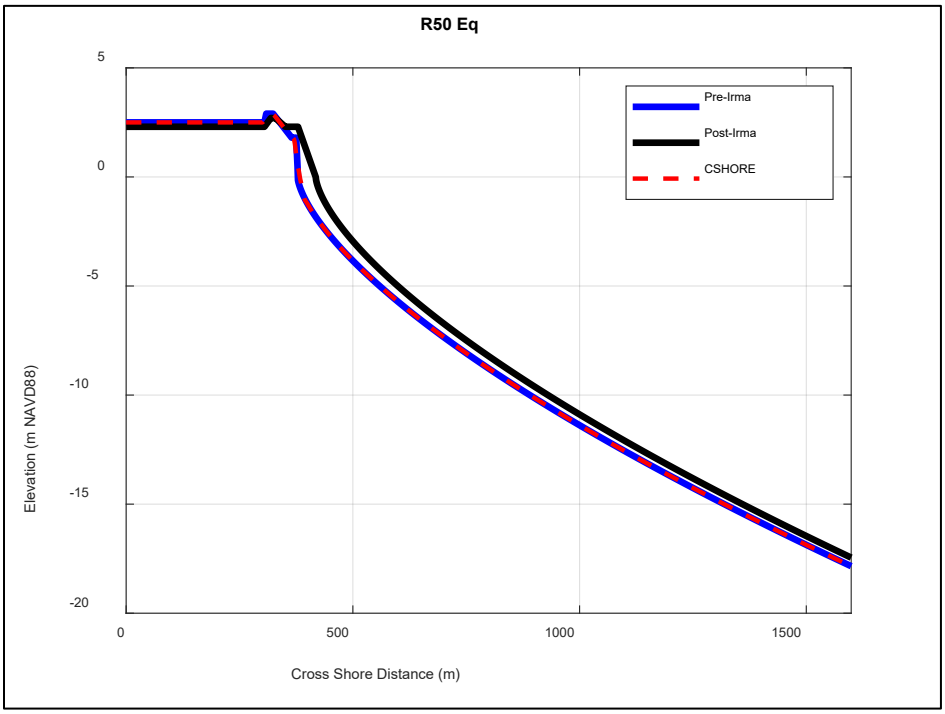

A 25

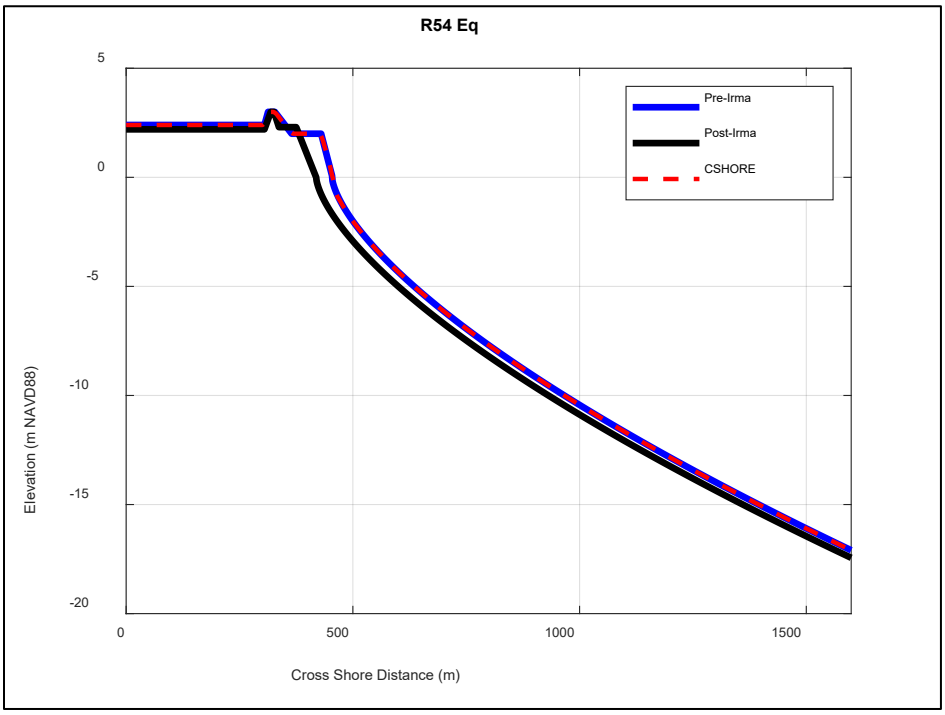

A 26

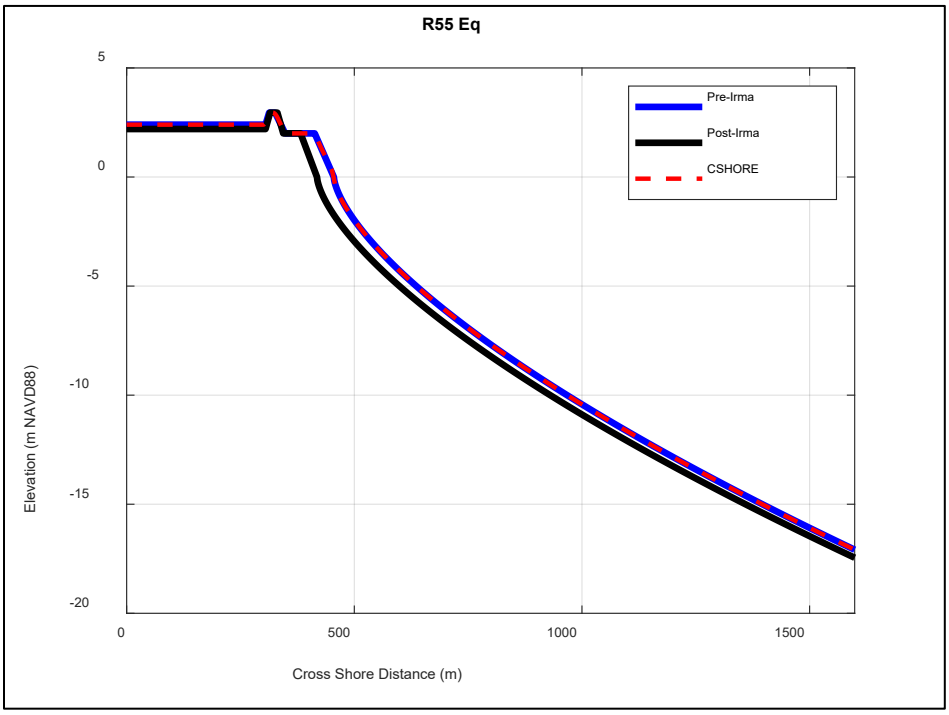
R55 Eq
Pre-Irma
Post-Irma
CSHORE
Elevation (m NAVD88)
Cross Shore Distance (m)
5
0
-5
-10
-15
-20
0
500
1000
1500

A 27